

FIG. 3. A) The total TUNEL-positive germinal cells per 20 circular seminiferous tubules in wild-type and *gad* mice on various postnatal days. In each group, the data represent the mean \pm SD ($n = 4$; * $P < 0.05$). B) The extent of apoptosis in 2-wk-old mice. i, wild-type mice; ii, *gad* mice. Green fluorescence, TUNEL-positive cells; red fluorescence, nuclei stained with propidium iodide. Magnification $\times 100$. Bar = 30 μ m.

Levels of Apoptotic Proteins During the First Round of Spermatogenesis

Germ cell apoptosis involves genes encoding various factors, such as *Trp53*, the *Bcl2* family, and *caspase*, which are targets for ubiquitination [29–31]. Our previous work demonstrated that the expression of antiapoptotic proteins (*Bcl2* family and XIAP) is significantly elevated following cryptorchid stress in *gad* mice [22]. To explore whether the germ cell apoptotic wave is associated with changes in the levels of proteins known to be associated with cell death or survival, Western blot analysis was performed on testicular lysates obtained from 7-, 14-, 21-, 28-, and 35-day-old wild-type and *gad* mice (Fig. 5). Levels of TRP53 and Bax proteins were strikingly elevated in 7-day-old mice but barely detectable on Day 35. Caspase-3 was also strikingly elevated in 7-day-old mice. Since TRP53 modulates Bax expression [22, 32], the observed up-regulation of Bax is consistent with elevated TRP53 levels during the early apoptotic wave. Expression of the antiapoptotic protein Bcl-xL was weaker in immature compared with mature testes. Levels of TRP53, Bax, and caspase-3 proteins were significantly decreased in 7- and 14-day-old *gad* mice relative to the levels observed in wild-type testes (Fig. 5B). By contrast, the level of Bcl-xL protein appeared to be up-regulated earlier in *gad* mice (at 28 days) than in wild-type mice (at 35 days) (Fig. 5B).

Assessment of Cauda Epididymidis and Spermatozoa Morphology in *gad* Mice

The cauda epididymidis from wild-type and *gad* mice were weighed, and the sperm were collected and analyzed. The cauda epididymidis from *gad* mice weighed significantly less, likely resulting from the lower sperm concentration measured in *gad* mice ($19.5 \times 10^6/\text{ml}$) compared with wild-type mice ($23.6 \times 10^6/\text{ml}$) (Table 1). Furthermore, abnormal sperm morphology, including head and midpiece defects or a detached head, occurred significantly

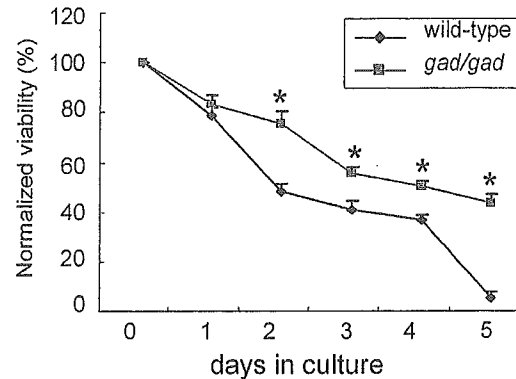


FIG. 4. In vitro survival of testicular germ cells. Testicular germ cells were isolated from wild-type and *gad* mice at 14 days of age. After culture, viability was determined using a Vi-Cell XR cell viability analyzer (Beckman Coulter). Viability at each time point was normalized to that at Day 0. Each data point represents the mean \pm SD ($n = 4$; * $P < 0.05$).

more often in *gad* mice (Table 1 and Fig. 6A). Immunocytochemical analysis showed that UCHL1 and ubiquitin were expressed in defective spermatozoa but not in normal spermatozoa (Fig. 6B). Ubiquitin, a marker for sperm abnormalities [33], was detected mainly in defective spermatozoa. However, despite a significantly elevated number of defective spermatozoa, ubiquitin expression in *gad* mouse spermatozoa was similar to that in wild-type mice (data not shown).

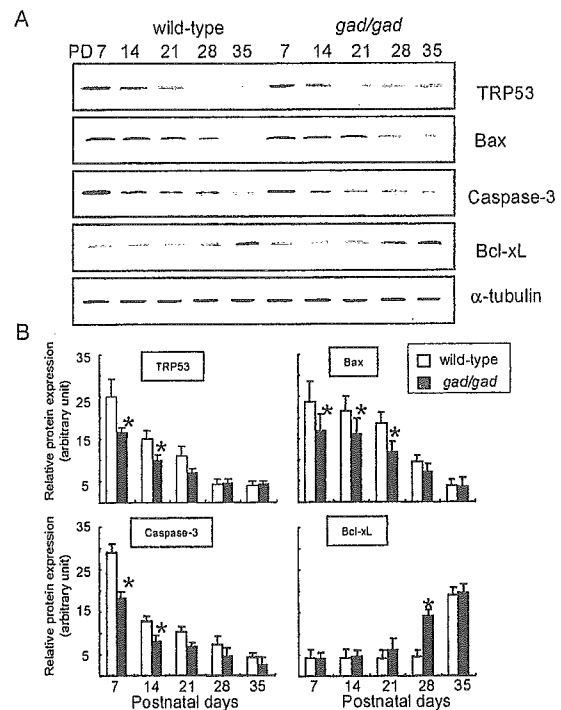


FIG. 5. A) Western blot analyses showing TRP53, Bax, caspase-3, and Bcl-xL levels in wild-type and *gad* mice during the first round of spermatogenesis. Protein (5 μ g/lane) was prepared from whole testes at 7, 14, 21, 28, and 35 days of age. Blots were reprobbed for α -tubulin to normalize for differences in the amount of protein loaded. Representative images of four independent experiments are shown. B) Quantitative Western blot analysis of changes in TRP53, Bax, caspase-3, and Bcl-xL levels. Relative protein expression (optical density) of the bands in panel A, normalized to α -tubulin. Each data point represents the mean \pm SD ($n = 4$; * $P < 0.05$).

TABLE 1. Analysis of epididymal tail weight and sperm morphology (mean ± SD) in 10-week-old wild-type and *gad* mice.

	Tail weight (mg)	Sperm concentration (10 ⁶ /ml)	Defect (%)			
			Head	Midpiece	Principal piece	Detached head
wild-type	30.0 ± 0.8	23.6 ± 3.7	7.2 ± 1.5	2.4 ± 1.3	1.1 ± 0.2	2.0 ± 1.0
<i>gad/gad</i>	24.7 ± 1.1*	19.5 ± 3.3*	14.1 ± 2.8*	4.7 ± 1.5*	1.7 ± 0.6	3.7 ± 1.2*

* Significantly different from wild-type mice (n = 7; P < 0.05).

Spermatozoa Motility in gad Mice

We measured sperm motility parameters in wild-type and *gad* mice. Of the parameters assessed, MSP, PMP, VAP (µm/sec), VSL (µm/sec), and VCL (µm/sec) were significantly lower in *gad* mice. ALH (µm), linearity (%), and straightness (%) did not differ significantly between *gad* and wild-type mice (Fig. 7). Of the parameters we measured, the number of PMP differed most significantly between *gad* mice (24.4%) and wild-type mice (34.3%) (Fig. 7A).

DISCUSSION

Spermatogenesis is a highly complex process involving male germ cell proliferation and maturation from spermatogonia to spermatozoa [34]. Apoptosis is common during this process and is believed to play an important role in controlling germ cell numbers and eliminating defective germ cells that carry DNA mutations, thus ensuring the production of intact, functional spermatozoa [35–37]. Normally, germ cells are extremely sensitive to DNA damage, as such lesions are incompatible with the ultimate function of these cells [23, 24, 37]. The early apoptotic wave may result in early elimination of defective germ cells in which DNA alterations have occurred through chromosomal crossing over during the first meiotic division [23, 24, 37].

Several lines of evidence indicate that UCHL1 associates with monoubiquitin and that the monoubiquitin pool is reduced in *gad* mice relative to wild-type mice [18, 19, 22]. Furthermore, testes from UCHL1-deficient *gad* mice [22] and mice carrying the K48R mutation in ubiquitin [38] show resistance to cryptorchid-induced apoptosis, suggesting that ubiquitin is critical for modulating testicular germ cell death. Normally, damaged proteins are polyubiquitinated and degraded via the ubiquitin-proteasome system; however, if damaged proteins are not degraded as easily

when monoubiquitin is either mutated or reduced [22, 38], then germinal cells may become resistant to programmed death. Our results with the *gad* mouse suggest that ubiquitin induction is important for regulating programmed germinal cell death that is normally observed during the first round of spermatogenesis. We have now shown that immature testes from *gad* mice are resistant to the massive wave of germinal cell apoptosis during the first round of spermatogenesis. The increased resistance of UCHL1-deficient germ cells to apoptosis-inducing conditions in vivo and in vitro suggests that UCHL1 is involved in spermatogenesis (Figs. 3 and 4). The activity of the ubiquitin-proteasome system may be required for specific transitions between multiple developmental cellular processes and sequential apoptosis during spermatogenesis [6, 7, 39]. In addition, the ubiquitin-proteasome system is required for the degradation or modification of numerous germ cell-specific proteins during different phases of spermatogenesis [39–41].

Early apoptosis in testicular germ cells is regulated by a complicated signal transduction pathway. The testes contain high levels of TRP53, Bcl2 family, and caspase-3 proteins, which are targets for ubiquitination [29–31, 42–45]. However, the involvement of the ubiquitin system in the regu-

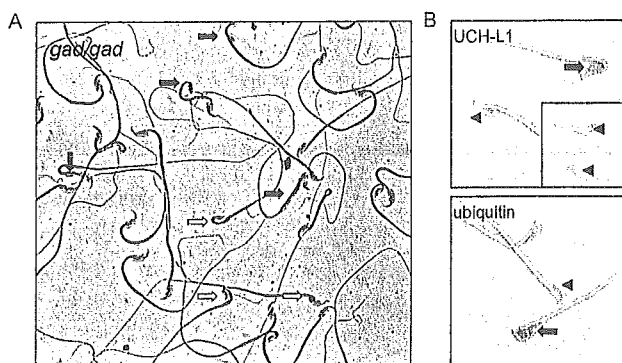


FIG. 6. A) Abnormal morphology of spermatozoa from *gad* mice. Spermatozoa were collected from the cauda epididymidis of 10-wk-old *gad* mice. Head defects (open arrows) and midpiece defects (closed arrows) are indicated. Magnification ×400. B) Immunocytochemistry of UCHL1 and ubiquitin in wild-type and *gad* mice. UCHL1- and ubiquitin-positive spermatozoa (closed arrows) and normal spermatozoa (both negative, arrowheads) in wild-type mice are indicated. The inset shows an image of spermatozoa from *gad* mice. Magnification ×1000.

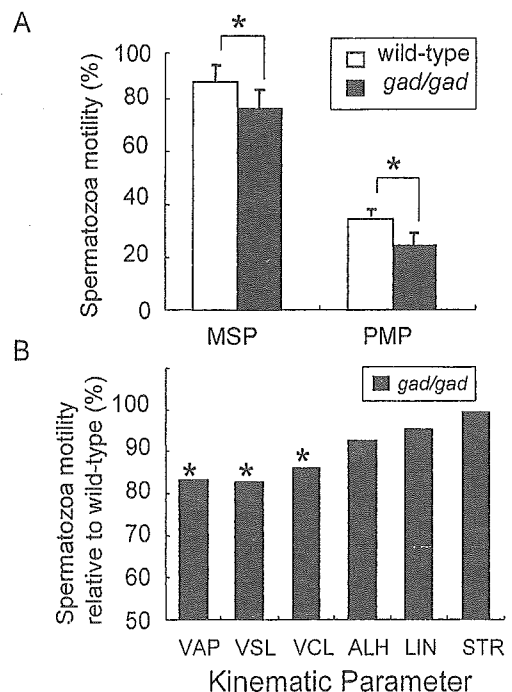


FIG. 7. Kinematic analysis of spermatozoa from the cauda epididymidis of 10-week-old wild-type and *gad* mice. A) Sperm motility. MSP, Percentage of motile sperm; PMP, Percentage of progressively motile sperm (n = 7; * P < 0.05). Data represent the mean ± SD. B) Movement characterization. VAP, Average path velocity (µm/sec); VSL, Straight-line velocity (µm/sec); VCL, Curvilinear velocity (µm/sec); ALH, Lateral head displacement (µm); LIN, Linearity (VSL/VCL × 100); STR, Straightness (VSL/VAP × 100). Data are expressed as a percentage of the values obtained for each parameter in wild-type mice (n = 7; * P < 0.05).

latory mechanisms of germ cell apoptosis has not been identified. A previous study showed that UCHL1-deficient *gad* mice express high levels of antiapoptotic proteins (Bcl2 family and XIAP) in the testis following cryptorchid-induced stress [22]. Alterations in the carefully maintained balance between the expression of apoptosis-inducing and apoptosis-protecting proteins may constitute one mechanism underlying the suppression of germ cell apoptosis observed in *gad* mice [46]. The decreased levels of TRP53, Bax, and caspase-3 observed in *gad* mice in this study are consistent with the suppression of germ cell apoptosis. In addition, the expression of the antiapoptotic protein Bcl-xL increased earlier in *gad* mice compared with wild-type mice. Therefore, the control of the apoptotic wave probably depends on variations in the balance between Bax and Bcl-xL [23, 47]. Analysis of the first round of spermatogenesis over time demonstrated a striking and massive wave of apoptotic germinal cells in 14-day-old mice (Fig. 3). High levels of UCHL1 protein were also observed at this age (Fig. 1) [20]. This early apoptotic wave was suppressed in the testes of *gad* mice, which had an abundance of germ cells compared with wild-type mice (Fig. 2). Moreover, the suppression of germ cell death is consistent with our previous report on cryptorchid stress injury in *gad* mice [22]. The testes of *gad* mice showed a phenotype similar to that of *Bax*-deficient mice or those overexpressing *Bcl2* or *Bcl-xL* [23, 25, 26]. Also, the testes of *Trp53*^{-/-} mice exhibited a similar phenotype involving decreased germ cell apoptosis and an increased number of germ cells [48].

In the present study, we also characterized spermatozoa in *gad* mice with regard to the following reproductive endpoints: 1) the weight of reproductive organs, 2) the concentration of sperm cells, and 3) the motility and morphology of spermatozoa collected from the cauda epididymidis. The weight of cauda epididymidis from *gad* mice was significantly lower compared with that from wild-type mice. The concentration of sperm cells was also significantly lower, and most motility parameters of spermatozoa collected from the cauda epididymidis were affected in *gad* mice (Fig. 7). The significant decline in progressive forward motility, VAP, VSL, and VCL indicates that UCHL1 deficiency affects not only the ability of spermatozoa to move in the forward direction but also their vigor. In addition, the percentage of morphologically abnormal spermatozoa was significantly higher in *gad* mice (Table 1 and Fig. 6A).

Sperm production in the testis is a regulated balance between germ cell division and germ cell loss [26, 49], and there is emerging evidence that the ubiquitin-proteasome system may be central to the coordination of this process. For example, during spermatogenesis, the general activity of the ubiquitin-proteasome system is high, probably reflecting the requirement for massive degradation of cytoplasmic and nuclear proteins [6, 7, 50, 51]. Additionally, mutation of the ubiquitin-conjugating enzyme HR6B results in impaired spermatogenesis during nuclear condensation in spermatids [39, 41]. We found the fact that UCHL1 associates with monoubiquitin in several lines of *gad* mice [18, 19, 22]. Furthermore, both proteins are expressed abundantly and at comparable levels in testis and the epididymis [11, 13, 14], suggesting that the functions of two proteins are important during spermatogenesis. Ubiquitin is present in defective spermatozoa, and proteins in these cells become ubiquitinated during epididymal passage (Fig. 6B) [11, 14, 33, 52, 53]. Furthermore, ubiquitination in the epididymis may trigger apoptotic mechanisms that recognize and eliminate abnormal spermatozoa [49, 54, 55].

Further study is required to elucidate the functional significance of the association between UCHL1 and ubiquitin during spermatozoa maturation in the epididymis. However, our observations suggest that UCHL1 may function to regulate sperm production and to ubiquitinate proteins in defective spermatozoa. Our present study demonstrates that UCHL1-deficient *gad* mice are resistant to the wave of germinal cell apoptosis that occurs during the first round of spermatogenesis and that these mice have defects in sperm production, motility, and morphology. These results suggest that UCHL1 functions in the early apoptotic wave during the first round of spermatogenesis and in the control of sperm quality during sperm maturation.

ACKNOWLEDGMENTS

We thank H. Kikuchi for technical assistance with tissue sections and M. Shikama for the care and breeding of animals.

REFERENCES

- Ciechanover A, Finley D, Varshavsky A. Ubiquitin dependence of selective protein degradation demonstrated in the mammalian cell cycle mutant ts85. *Cell* 1984; 37:57-66.
- Glotzer M, Murray AW, Kirschner MW. Cyclin is degraded by the ubiquitin pathway. *Nature* 1991; 349:132-138.
- Strous GJ, Govers R. The ubiquitin-proteasome system and endocytosis. *J Cell Sci* 1999; 112(pt 10):1417-1423.
- Wilkinson KD. Regulation of ubiquitin-dependent processes by deubiquitinating enzymes. *FASEB J* 1997; 11:1245-1256.
- Hershko A, Ciechanover A. The ubiquitin system. *Annu Rev Biochem* 1998; 67:425-479.
- Baarends WM, Roest HP, Grootegoed JA. The ubiquitin system in gametogenesis. *Mol Cell Endocrinol* 1999; 151:5-16.
- Baarends WM, van der Laan R, Grootegoed JA. Specific aspects of the ubiquitin system in spermatogenesis. *J Endocrinol Invest* 2000; 23:597-604.
- Ciechanover A. The ubiquitin-proteasome pathway: on protein death and cell life. *EMBO J* 1998; 17:7151-7160.
- Weissman AM. Themes and variations on ubiquitylation. *Nat Rev Mol Cell Biol* 2001; 2:169-178.
- Wing SS. Deubiquitinating enzymes—the importance of driving in reverse along the ubiquitin-proteasome pathway. *Int J Biochem Cell Biol* 2003; 35:590-605.
- Fraile B, Martin R, De Miguel MP, Arenas MI, Bethencourt FR, Peinado F, Paniagua R, Santamaria L. Light and electron microscopic immunohistochemical localization of protein gene product 9.5 and ubiquitin immunoreactivities in the human epididymis and vas deferens. *Biol Reprod* 1996; 55:291-297.
- Kon Y, Endoh D, Iwanaga T. Expression of protein gene product 9.5, a neuronal ubiquitin C-terminal hydrolase, and its developing change in sertoli cells of mouse testis. *Mol Reprod Dev* 1999; 54:333-341.
- Kwon J, Kikuchi T, Setsuie R, Ishii Y, Kyuwa S, Yoshikawa Y. Characterization of the testis in congenitally ubiquitin carboxy-terminal hydrolase-1 (Uch-L1) defective (*gad*) mice. *Exp Anim* 2003; 52:1-9.
- Martin R, Santamaria L, Fraile B, Paniagua R, Polak JM. Ultrastructural localization of PGP 9.5 and ubiquitin immunoreactivities in rat ductus epididymidis epithelium. *Histochem J* 1995; 27:431-439.
- Pickart CM, Rose IA. Ubiquitin carboxyl-terminal hydrolase acts on ubiquitin carboxyl-terminal amides. *J Biol Chem* 1985; 260:7903-7910.
- Liu Y, Fallon L, Lashuel HA, Liu Z, Lansbury PT, Jr. The UCH-L1 gene encodes two opposing enzymatic activities that affect alpha-synuclein degradation and Parkinson's disease susceptibility. *Cell* 2002; 111:209-218.
- Liu Y, Lashuel HA, Choi S, Xing X, Case A, Ni J, Yeh LA, Cuny GD, Stein RL, Lansbury PT, Jr. Discovery of inhibitors that elucidate the role of UCH-L1 activity in the H1299 lung cancer cell line. *Chem Biol* 2003; 10:837-846.
- Osaka H, Wang YL, Takada K, Takizawa S, Setsuie R, Li H, Sato Y, Nishikawa K, Sun YJ, Sakurai M, Harada T, Hara Y, Kimura I, Chiba S, Namikawa K, Kiyama H, Noda M, Aoki S, Wada K. Ubiquitin carboxy-terminal hydrolase L1 binds to and stabilizes monoubiquitin in neuron. *Hum Mol Genet* 2003; 12:1945-1958.

19. Harada T, Harada C, Wang YL, Osaka H, Amanai K, Tanaka K, Takizawa S, Setsuie R, Sakurai M, Sato Y, Noda M, Wada K. Role of ubiquitin carboxy terminal hydrolase-L1 in neural cell apoptosis induced by ischemic retinal injury in vivo. *Am J Pathol* 2004; 164:59-64.
20. Kwon J, Wang YL, Setsuie R, Sekiguchi S, Sakurai M, Sato Y, Lee WW, Ishii Y, Kyuwa S, Noda M, Wada K, Yoshikawa Y. Developmental regulation of ubiquitin C-terminal hydrolase isozyme expression during spermatogenesis in mice. *Biol Reprod* 2004; 71:515-521.
21. Saigoh K, Wang YL, Suh JG, Yamanishi T, Sakai Y, Kiyosawa H, Harada T, Ichihara N, Wakana S, Kikuchi T, Wada K. Intragenic deletion in the gene encoding ubiquitin carboxy-terminal hydrolase in gad mice. *Nat Genet* 1999; 23:47-51.
22. Kwon J, Wang YL, Setsuie R, Sekiguchi S, Sato Y, Sakurai M, Noda M, Aoki S, Yoshikawa Y, Wada K. Two closely related ubiquitin C-terminal hydrolase isozymes function as reciprocal modulators of germ cell apoptosis in cryptorchid testis. *Am J Pathol* 2004; 165:1367-1374.
23. Rodriguez I, Ody C, Araki K, Garcia I, Vassalli P. An early and massive wave of germinal cell apoptosis is required for the development of functional spermatogenesis. *EMBO J* 1997; 16:2262-2270.
24. Jahnukainen K, Chrysis D, Hou M, Parvinen M, Eksborg S, Soder O. Increased apoptosis occurring during the first wave of spermatogenesis is stage-specific and primarily affects midpachytene spermatocytes in the rat testis. *Biol Reprod* 2004; 70:290-296.
25. Furuchi T, Masuko K, Nishimune Y, Obinata M, Matsui Y. Inhibition of testicular germ cell apoptosis and differentiation in mice misexpressing Bcl-2 in spermatogonia. *Development* 1996; 122:1703-1709.
26. Russell LD, Chiarini-Garcia H, Korsmeyer SJ, Knudson CM. Bax-dependent spermatogonia apoptosis is required for testicular development and spermatogenesis. *Biol Reprod* 2002; 66:950-958.
27. Slott VL, Suarez JD, Perreault SD. Rat sperm motility analysis: methodologic considerations. *Reprod Toxicol* 1991; 5:449-458.
28. Goyal HO, Braden TD, Mansour M, Williams CS, Kamaleldin A, Srivastava KK. Diethylstilbestrol-treated adult rats with altered epididymal sperm numbers and sperm motility parameters, but without alterations in sperm production and sperm morphology. *Biol Reprod* 2001; 64:927-934.
29. Chipuk JE, Green DR. Cytoplasmic p53: Bax and forward. *Cell Cycle* 2004; 3:429-431.
30. Dimmeler S, Breitschopf K, Haendeler J, Zeiher AM. Dephosphorylation targets Bcl-2 for ubiquitin-dependent degradation: a link between the apoptosome and the proteasome pathway. *J Exp Med* 1999; 189:1815-1822.
31. Suzuki Y, Nakabayashi Y, Takahashi R. Ubiquitin-protein ligase activity of X-linked inhibitor of apoptosis protein promotes proteasomal degradation of caspase-3 and enhances its anti-apoptotic effect in Fas-induced cell death. *Proc Natl Acad Sci U S A* 2001; 98:8662-8667.
32. Selvakumaran M, Lin HK, Miyashita T, Wang HG, Krajewski S, Reed JC, Hoffman B, Liebermann D. Immediate early upregulation of bax expression by p53 but not TGF beta 1: a paradigm for distinct apoptotic pathways. *Oncogene* 1994; 9:1791-1798.
33. Sutovsky P, Moreno R, Ramalho-Santos J, Dominko T, Thompson WE, Schatten G. A putative, ubiquitin-dependent mechanism for the recognition and elimination of defective spermatozoa in the mammalian epididymis. *J Cell Sci* 2001; 114:1665-1675.
34. de Kretser DM, Loveland KL, Meinhardt A, Simorangkir D, Wreford N. Spermatogenesis. *Hum Reprod* 1998; 13(suppl 1):1-8.
35. Gosden R, Spears N. Programmed cell death in the reproductive system. *Br Med Bull* 1997; 53:644-661.
36. Matsui Y. Regulation of germ cell death in mammalian gonads. *APMIS* 1998; 106:142-147. Discussion 147-148.
37. Print CG, Loveland KL. Germ cell suicide: new insights into apoptosis during spermatogenesis. *Bioessays* 2000; 22:423-430.
38. Rasoulpour RJ, Schoenfeld HA, Gray DA, Boekelheide K. Expression of a K48R mutant ubiquitin protects mouse testis from cryptorchid injury and aging. *Am J Pathol* 2003; 163:2595-2603.
39. Baarends WM, Wassenaar E, Hoogerbrugge JW, van Cappellen G, Roest HP, Vreeburg J, Ooms M, Hoeijmakers JH, Grootegoed JA. Loss of HR6B ubiquitin-conjugating activity results in damaged synaptonemal complex structure and increased crossing-over frequency during the male meiotic prophase. *Mol Cell Biol* 2003; 23:1151-1162.
40. Baarends WM, Hoogerbrugge JW, Roest HP, Ooms M, Vreeburg J, Hoeijmakers JH, Grootegoed JA. Histone ubiquitination and chromatin remodeling in mouse spermatogenesis. *Dev Biol* 1999; 207:322-333.
41. Roest HP, van Klaveren J, de Wit J, van Gurp CG, Koken MH, Vermeij M, van Roijen JH, Hoogerbrugge JW, Vreeburg JT, Baarends WM, Bootsma D, Grootegoed JA, Hoeijmakers JH. Inactivation of the HR6B ubiquitin-conjugating DNA repair enzyme in mice causes male sterility associated with chromatin modification. *Cell* 1996; 86:799-810.
42. Marshansky V, Wang X, Bertrand R, Luo H, Duguid W, Chinnadurai G, Kanaan N, Vu MD, Wu J. Proteasomes modulate balance among proapoptotic and antiapoptotic Bcl-2 family members and compromise functioning of the electron transport chain in leukemic cells. *J Immunol* 2001; 166:3130-3142.
43. Oren M. Regulation of the p53 tumor suppressor protein. *J Biol Chem* 1999; 274:36031-36034.
44. Orłowski RZ. The role of the ubiquitin-proteasome pathway in apoptosis. *Cell Death Differ* 1999; 6:303-313.
45. Yang Y, Yu X. Regulation of apoptosis: the ubiquitous way. *FASEB J* 2003; 17:790-799.
46. Beumer TL, Roepers-Gajadien HL, Gademan IS, Lock TM, Kal HB, De Rooij DG. Apoptosis regulation in the testis: involvement of Bcl-2 family members. *Mol Reprod Dev* 2000; 56:353-359.
47. Borner C. The Bcl-2 protein family: sensors and checkpoints for life-or-death decisions. *Mol Immunol* 2003; 39:615-647.
48. Yin Y, Stahl BC, DeWolf WC, Morgentaler A. p53-mediated germ cell quality control in spermatogenesis. *Dev Biol* 1998; 204:165-171.
49. Sutovsky P. Ubiquitin-dependent proteolysis in mammalian spermatogenesis, fertilization, and sperm quality control: killing three birds with one stone. *Microsc Res Tech* 2003; 61:88-102.
50. Rajapurohitam V, Bedard N, Wing SS. Control of ubiquitination of proteins in rat tissues by ubiquitin conjugating enzymes and isopeptidases. *Am J Physiol Endocrinol Metab* 2002; 282:E739-E745.
51. Rajapurohitam V, Morales CR, El-Alfy M, Lefrancois S, Bedard N, Wing SS. Activation of a UBC4-dependent pathway of ubiquitin conjugation during postnatal development of the rat testis. *Dev Biol* 1999; 212:217-228.
52. Lippert TH, Seeger H, Schieferstein G, Voelter W. Immunoreactive ubiquitin in human seminal plasma. *J Androl* 1993; 14:130-131.
53. Sutovsky P, Terada Y, Schatten G. Ubiquitin-based sperm assay for the diagnosis of male factor infertility. *Hum Reprod* 2001; 16:250-258.
54. Sinha Hikim AP, Swerdloff RS. Hormonal and genetic control of germ cell apoptosis in the testis. *Rev Reprod* 1999; 4:38-47.
55. Sutovsky P, Hauser R, Sutovsky M. Increased levels of sperm ubiquitin correlate with semen quality in men from an andrology laboratory clinic population. *Hum Reprod* 2004; 19:628-638.

Akt/PKB Regulates Actin Organization and Cell Motility via Girdin/APE

Atsushi Enomoto,¹ Hideki Murakami,¹ Naoya Asai,¹ Nobuhiro Morone,^{2,5} Takashi Watanabe,³ Kumi Kawai,⁴ Yoshiki Murakumo,¹ Jiro Usukura,² Kozo Kaibuchi,³ and Masahide Takahashi^{1,4,*}

¹Department of Pathology

²Department of Cell Biology and Anatomy

³Department of Cell Pharmacology

⁴Division of Molecular Pathology

Center for Neurological Disease and Cancer

Nagoya University Graduate School of Medicine

65 Tsurumai-cho

Showa-ku, Nagoya

Aichi 466-8550

Japan

⁵Department of Ultrastructural Research

National Institute of Neuroscience

National Center of Neurology and Psychiatry

Kodaira

Tokyo 187-8502

Japan

Summary

The serine/threonine kinase Akt (also called protein kinase B) is well known as an important regulator of cell survival and growth and has also been shown to be required for cell migration in different organisms. However, the mechanism by which Akt functions to promote cell migration is not understood. Here, we identify an Akt substrate, designated Girdin/APE (Akt-phosphorylation enhancer), which is an actin binding protein. Girdin expresses ubiquitously and plays a crucial role in the formation of stress fibers and lamellipodia. Akt phosphorylates serine at position 1416 in Girdin, and phosphorylated Girdin accumulates at the leading edge of migrating cells. Cells expressing mutant Girdin, in which serine 1416 was replaced with alanine, formed abnormal elongated shapes and exhibited limited migration and lamellipodia formation. These findings suggest that Girdin is essential for the integrity of the actin cytoskeleton and cell migration and provide a direct link between Akt and cell motility.

Introduction

In multicellular organisms, cell migration is a highly integrated process that orchestrates embryonic morphogenesis, contributes to tissue repair and regeneration, and drives disease progression in cancer, atherosclerosis, and immune diseases (Lauffenburger and Horwitz, 1996; Ridley et al., 2003). Cell migration that is initiated in response to multiple extracellular cues such as growth factors and cell-extracellular matrix adhesions requires dynamic and spatially regulated changes of the actin cytoskeleton, microtubules, adhesion mole-

cules, and extracellular matrix. This function is mediated and coordinated by many different intracellular signaling molecules, including the Rho family of small GTPases, Ca²⁺-regulated proteins, mitogen-activated protein kinases (MAPKs), protein kinase C, phosphatidylinositol kinases, and tyrosine kinases (Etienne-Manneville and Hall, 2002; Ridley, 2001).

Akt, also known as protein kinase B (PKB), is a serine/threonine kinase activated downstream of class I phosphatidylinositol 3-kinase (PI3K) and various receptors. It has emerged as the key regulator for many signal transduction pathways, modulating multiple processes such as cell survival, proliferation, growth, angiogenesis, and glucose metabolism (Brazil et al., 2002; Datta et al., 1999; Vivanco and Sawyers, 2002). Akt substrates include transcription factors, antiapoptotic proteins, and protein kinases that regulate protein synthesis. In addition, Akt has also been shown to be required for chemotaxis in mammalian leukocytes and *Dictyostelium* cells (Chung et al., 2001; Meili et al., 1999; Merlot and Firtel, 2003). A growing body of evidence indicates that Akt promotes cell motility in mammalian fibroblasts and tumor cells (Higuchi et al., 2001; Kim et al., 2001; Morales-Ruiz et al., 2000). PI3K and the tumor suppressor protein PTEN, upstream regulators of Akt activity, have been shown to be essential for cell migration and the establishment of cell polarity (Merlot and Firtel, 2003). Moreover, clinical studies have revealed that cancer patients whose tumors have increased Akt expression tend to have more invasive and metastatic diseases, which are associated with a poor prognosis (Scheid and Woodgett, 2001; Vivanco and Sawyers, 2002). These findings indicate that Akt is involved in cell migration and invasion in cells of many different organisms. However, the molecular mechanisms of how Akt regulates the cytoskeleton and thereby modulates cell motility are largely unknown. The localization of the pleckstrin-homology (PH) domain of Akt at the leading edge during chemotaxis in neutrophils (Servant et al., 2000), *Dictyostelium* cells (Meili et al., 1999), and mammalian fibroblasts (Higuchi et al., 2001) suggests that this kinase phosphorylates and regulates yet to be identified proteins that are involved in remodeling of the leading edge (Merlot and Firtel, 2003).

In eukaryotic cells, the integrity and dynamic reorganization of the actin cytoskeleton are essential for cellular morphogenesis and generation of the forces needed for motility. Actin bundles provide tensile strength, whereas the crosslinked three-dimensional orthogonal networks provide elasticity (Stossel et al., 2001). At the leading edge, migrating cells create short-branched actin networks in order to sustain a pushing force (Pollard and Borisy, 2003). These features of the actin cytoskeleton are regulated by multiple actin filament cross-linking/bundling proteins that include the fimbrin/ α -actinin/filamin (also termed ABP-280), villin, scruin, and fascin families (Pollard, 2002; Revenu et al., 2004). Although each actin crosslinking protein has a distinct function that is essential for normal physiology, appar-

*Correspondence: mtakaha@med.nagoya-u.ac.jp

ent redundancy of these proteins has been suggested (Pollard, 2002). Organisms or cells that lack some actin crosslinking proteins still survive despite large defects in cell behavior and growth rate. *Dictyostelium* cells that lacked α -actinin showed no motility defects, with deficiencies only in behavior and architecture (Pollard, 2002; Rivero et al., 1996; Stossel et al., 2001). A cell line established from human malignant melanoma, which expressed no filamin, could not undergo locomotion in response to growth factors but was still able to survive (Stossel et al., 2001). These findings suggest that these crosslinking proteins share overlapping functions in the actin system, and that the inventory of important actin crosslinking proteins may still be incomplete (Pollard, 2002).

In this study, we identified a novel, to our knowledge, substrate of Akt. We designate it Girdin (girders of actin filaments), because RNA interference (RNAi)-mediated depletion of Girdin gives rise to the disruption of stress fibers and limited extension of lamellipodia in fibroblasts. A recently published paper also identified the same protein designated APE (Akt-phosphorylation enhancer) as an Akt binding protein (Anai et al., 2005), although a role in actin organization was not characterized. We show that the phosphorylation of Girdin/APE by Akt occurs at the leading edge of migrating cells, which controls the association between Girdin and the plasma membrane and subsequently facilitates the formation of lamellipodium.

Results

Identification of an Akt-Interacting Protein, Girdin/APE

To identify novel Akt substrates, we performed a yeast two-hybrid screen with full-length human Akt1 as bait and searched for interacting proteins by using a human fetal brain cDNA library. Two independent and overlapping clones (F-10 and F-12) encoding a novel gene product were identified. When expressed in yeast, the protein encoded by the F-10 and F-12 cDNAs was shown to interact only with the carboxyl-terminal regulatory domain (RD) of Akt1 (Figures 1A and 1B). Use of 5'-rapid amplification of cDNA ends (5'-RACE) provided a clone comprising the entire coding region with an additional 3.8 kb cDNA of contiguous 5' sequence. The full-length cDNA included an open reading frame of 5610 base pairs (bp) and was predicted to encode a novel, to our knowledge, protein of 1870 amino acids, which we designated Girdin, with a calculated molecular mass of 220 kilodaltons (kDa) (Figure S1; see the Supplemental Data available with this article online). Database searches revealed homologs in mouse, rat, and *Drosophila* (not shown), but no apparent matches in *Caenorhabditis elegans* and *Dictyostelium*. A mouse ortholog of Girdin named APE was recently reported (Anai et al., 2005).

The structure of Girdin predicted by the COILS algorithm (Lupas et al., 1991) showed a tendency to assume an α -helical coiled-coil conformation in its middle domain, between Ala-253 and Lys-1375, with a high coiled-coil probability of 1.0 (Figure 1C). The predicted coiled-coil domain contains 135 continuous heptad re-

peats ([*abcdefg*]₁₃₅) that are typical of α -helical coiled-coils (Figure S1). The 9.5 kb Girdin transcript was found to be expressed ubiquitously in various human tissues by high-stringency Northern blot analysis (Figure 1D). To facilitate further studies on Girdin, we generated a polyclonal antibody (Ab) raised against its 19 C-terminal amino acids. Western blot analysis revealed that the anti-Girdin Ab recognizes a specific band of relative molecular mass of 250 kDa in human brain and testis lysates (Figure 1E).

Because of the existence of an α -helical coiled-coil domain in the primary structure of Girdin, we investigated the possibility of Girdin being an oligomeric molecule. Cell lysates from COS7 cells were analyzed by Western blot analysis with anti-Girdin Ab, either directly or after crosslinking with 100 μ M Bis(sulfosuccinimidyl) suberate (BS³) (Figure 1F). In the presence of BS³, Girdin was predominantly found in a complex of large molecular mass. To determine the molecular mass of Girdin-containing protein complexes in intact cells, we subjected the lysates from COS7 cells to gel filtration (Figure S2). The data confirmed that Girdin forms a large protein complex. We next tested whether the NT and CT domains contribute to the oligomerization of Girdin. When V5 epitope-tagged NT (NT-V5) and myc epitope-tagged NT (NT-myc) were expressed in COS7 cells, a complex of these two NT domains was observed (Figure 1G). This result implies that the NT domain facilitates the oligomerization of Girdin. In contrast, the CT domain did not form an oligomer in cells (data not shown). Analysis of the lysates from COS7 cells expressing the NT domain by gel filtration suggested that the NT domain forms a dimer (Figure S2).

Akt Phosphorylates Girdin In Vitro and In Vivo

We initially used in vitro and in vivo assays to ascertain if Girdin and Akt physically interact with each other. Neither in vitro binding nor immunoprecipitation assays with various fragments of Girdin and Akt demonstrated the formation of a stable complex of the two proteins (data not shown), suggesting that they may normally associate in a very transient manner, as observed for the interactions between protein kinases and their substrates (Brazil et al., 2002). Although Anai et al. (2005) observed a weak association of the two proteins by immunoprecipitation, the difference may be due to the experimental conditions used.

It has been established that Akt preferentially phosphorylates substrates that contain the sequence R-x-R-x-x-S/T (Alessi et al., 1996). The amino acid sequence adjacent to a serine at position 1416 (Ser-1416 indicated by the underlined "S," RERQKS) in the CT domain of Girdin conforms to this consensus sequence (Figure 2Aa). This is the only consensus site in the protein. Since the CT domain with the putative phosphorylation site is conserved in different mammalian Girdin homologs (data not shown), we asked whether Akt phosphorylates Girdin. An in vitro kinase assay revealed that Girdin CT wild-type (WT), but not its Ser \rightarrow Ala mutant (SA), was phosphorylated by active Akt, indicating that Akt directly phosphorylates the Ser-1416 in vitro (Figure 2Ab). In contrast, neither the NT nor the coiled-coil domain of Girdin was phosphorylated by Akt in vitro (Figure 2B).

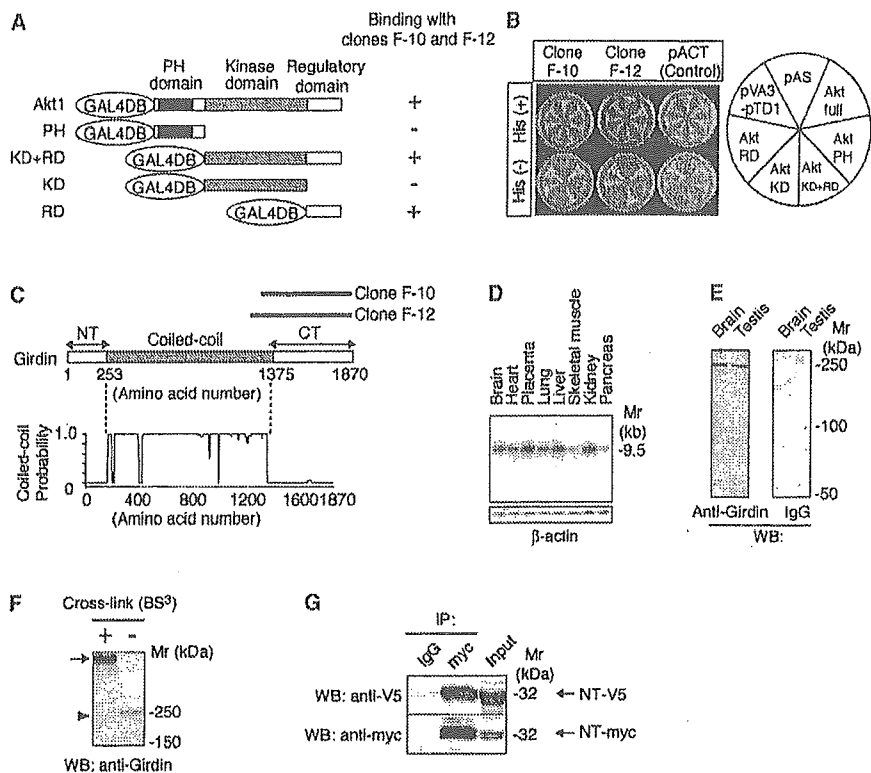


Figure 1. Identification, Primary Structure, and Expression of Girdin

(A) Schematic illustration of bait constructs for yeast two-hybrid binding assays. The cDNA fragments corresponding to the indicated domains of human Akt1 were fused in frame to the DNA binding domain of GAL4 transcription factor (GAL4DB) in the pAS2 vector. PH, pleckstrin homology domain; KD, catalytic kinase domain; RD, regulatory domain.

(B) Interactions of clones F-10 and F-12 with human Akt1 in yeast two-hybrid binding assays. pAS, a negative control; pVA3-pTD1, a positive control; His, histidine.

(C) Schematic presentation of Girdin and structure predictions provided by the COILS algorithm.

(D) Ubiquitous expression of Girdin mRNA in human adult tissues. A human multiple-tissue Northern (MTN) blot (Clontech) was hybridized with a probe corresponding to the 3' region of Girdin cDNA.

(E) Endogenous Girdin in lysates from human brain and testis was detected with anti-Girdin polyclonal antibody, but not with rabbit IgG, under reducing conditions.

(F) Detection of a large complex formation by endogenous Girdin. COS7 postnuclear supernatants were subjected to Western blot analysis by using anti-Girdin antibody, either directly (-) or after crosslinking with 100 μ M BS³ (+). The size of a band detected after crosslinking (arrow) is extremely large compared with that without crosslinking (arrowhead).

(G) The NT domain of Girdin forms an oligomer. NT-V5 and NT-myc were transfected into COS7 cells and immunoprecipitated with anti-myc antibody. NT-V5 was coimmunoprecipitated with NT-myc. The multiple bands in the lower panel may represent the degradation of NT-myc in cells.

In order to confirm that Ser-1416 is the site of Akt-catalyzed phosphorylation *in vivo*, we raised an antibody to a peptide that includes phosphorylated Ser-1416 and used it for Western blotting (Figure 2C). The anti-phospho Ser-1416 peptide antibody (anti-P-Girdin Ab) recognized the Girdin CT (WT) that was coexpressed with wild-type (Akt WT) or constitutively active Akt (Akt CA), but not with dominant-negative Akt (Akt DN). The anti-P-Girdin Ab did not recognize the Girdin CT (SA) mutant coexpressed with the Akt CA. These findings indicate that the anti-P-Girdin Ab specifically recognizes the Girdin CT phosphorylated at Ser-1416.

We next asked whether the anti-P-Girdin Ab can detect the endogenous Girdin phosphorylated in response to external stimuli that physiologically activate

endogenous Akt. As shown in Figure 2D, the addition of epidermal growth factor (EGF) induced the phosphorylation of a protein that corresponds to immunoprecipitated Girdin (250 kDa) with a time course similar to that of Akt activation. In addition, the phosphorylation of Girdin was inhibited when cells were treated with the PI3K inhibitors LY294002 and Wortmannin, but not with the mitogen-activated protein kinase kinase 1 (MEK1) inhibitor PD98059. We therefore concluded that the phosphorylation of Girdin is induced by EGF in a PI3K-dependent manner. The expression of Akt WT and Akt CA, but not Akt DN, induced significant phosphorylation of Girdin (Figure 2E), indicating that active Akt alone is sufficient to induce its phosphorylation in cells. Moreover, Girdin phosphorylation was undetectable in

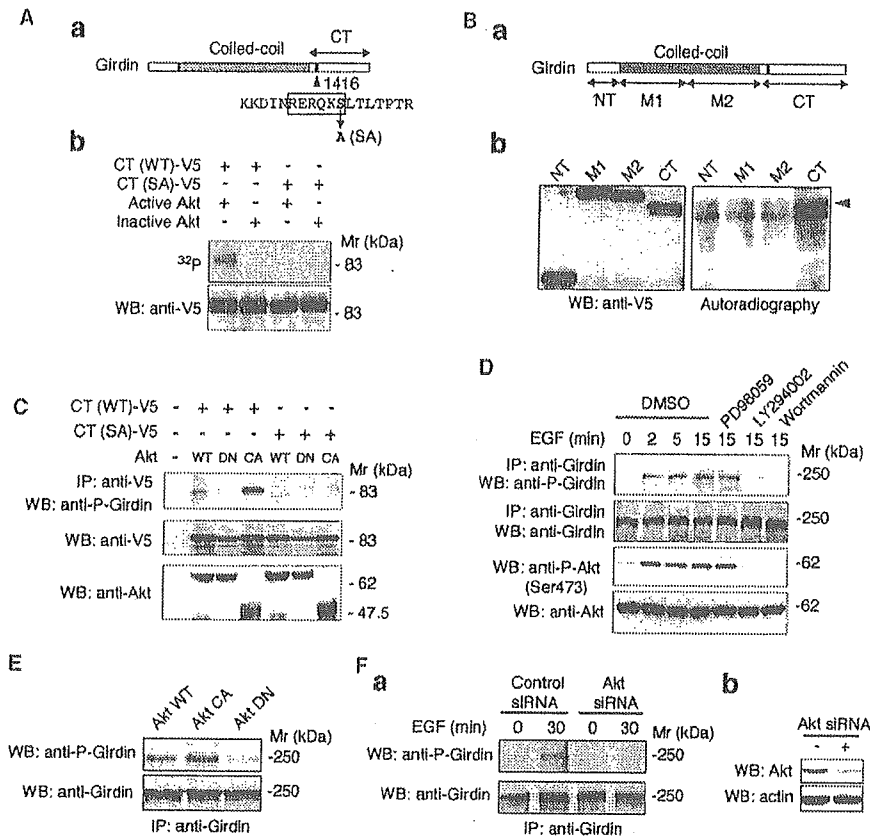


Figure 2. Akt Phosphorylates Girdin In Vitro and In Vivo

(A) (Aa) A potential Akt phosphorylation site at serine 1416 of the Girdin CT domain. (Ab) Girdin CT-V5, WT or SA (serine 1416 replaced with alanine), was transfected into COS7 cells and immunoprecipitated with anti-V5 antibody, followed by incubation with recombinant active or inactive Akt in the presence of [γ - 32 P]ATP. Phosphorylated Girdin CT was detected by autoradiography (upper panel). Immunoprecipitated Girdin CTs were detected by Western blot analysis (lower panel).

(B) Various fragments of Girdin (Ba) tagged with V5 were transfected into COS7 cells and immunoprecipitated with anti-V5 antibody, followed by (Bb) incubation with recombinant active Akt in the presence of [γ - 32 P]ATP. Phosphorylated Girdin CT was detected by autoradiography (right panel). Immunoprecipitated fragments were detected by Western blot analysis (left panel).

(C) COS7 cells were cotransfected with Girdin CT-V5 (WT or SA) and Akt mutants. Immunoprecipitates with anti-V5 antibody were subjected to Western blot analysis with anti-phospho Girdin (anti-P-Girdin) antibody (upper panel). Expression of Girdin CTs and Akt mutants was monitored by Western blot analyses (middle and lower panels).

(D) COS7 cells were stimulated with EGF (50 ng/ml) for 15 min in the presence of DMSO (0.1%), PD98059 (50 μ M), LY294002 (10 μ M), and Wortmannin (30 nM). Immunoprecipitates with anti-Girdin antibody were subjected to Western blot analyses with anti-P-Girdin and anti-Girdin antibodies. Activation of Akt was monitored by Western blot analyses with anti-phospho Akt antibody.

(E) COS7 cells were transfected with Akt mutants. Endogenous Girdin was immunoprecipitated with anti-Girdin antibody, followed by Western blot analyses with anti-P-Girdin (upper panel) and anti-Girdin (lower panel) antibodies.

(F) Effects of Akt knockdown on phosphorylation of endogenous Girdin. (Fa) COS7 cells were transfected with either control or Akt siRNAs and were incubated for 48 hr. Cells were then stimulated with EGF (50 ng/ml) for 30 min, and the phosphorylation of Girdin was analyzed as described in (E). (Fb) Depletion of Akt in COS7 cells by siRNA.

the cells transfected with Akt small interfering RNA (Akt siRNA) (Figure 2F). These findings confirmed that Akt activation is necessary for Girdin phosphorylation.

Girdin Associates with Actin Filaments via Its C-Terminal Domain

To determine the subcellular localization of Girdin, we immunofluorescently stained Vero fibroblasts with the anti-Girdin Ab. The results showed that Girdin was colocalized with the actin stress fibers in quiescent cells (Figure 3Aa). When the cells were stimulated with EGF (50 ng/ml), they started to polarize, followed by direc-

tional extension of lamellipodia. In the EGF-stimulated cells, Girdin localized not only on the actin stress fibers, but also on the lamellipodia at the leading edge, which was illustrated upon staining for the Arp2/3 binding protein Cortactin (Figure 3Ab).

The localization of Girdin raises the possibility that Girdin is an F-actin (filamentous actin) binding protein. To identify the actin binding domain of Girdin, we generated green fluorescence protein (GFP)-fused, truncated versions encoding the NT (GFP-NT), the N-terminal half (GFP-M1) and the C-terminal half (GFP-M2) of the coiled-coil domain, and the N-terminal half (GFP-

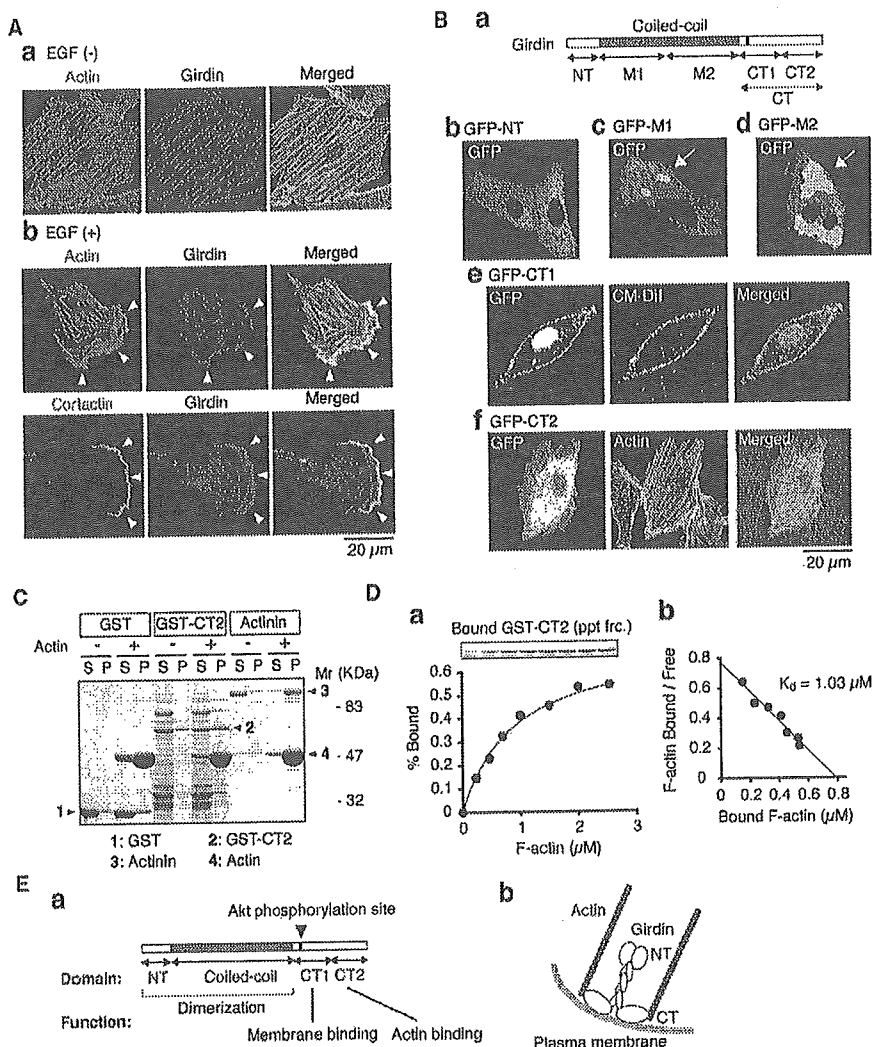


Figure 3. Girdin Binds to Actin Filaments through Its C-Terminal Domain

(A) (Aa) Quiescent or (Ab) EGF (50 ng/ml)-stimulated Vero cells were doubly stained with either Alexa488-phalloidin (upper panel) or anti-Cortactin antibody (lower panel) and anti-Girdin antibody. Arrowheads denote lamellipodia at the leading edge. (B) Subcellular localization of Girdin fragments. Various fragments of Girdin (Ba) fused with GFP were expressed in Vero cells, fixed, and stained with the (Bb–Bf) indicated probes. Arrows denote aggregates of the expressed proteins. CM-Dil, Chloromethylbenzamide. (C) Girdin CT2 directly interacts with filamentous actin in vitro. Purified GST (1), GST-CT2 (2), and α -actinin (3) were incubated with (+) or without (-) in vitro-prepared actin filaments (4). F-actin was subsequently pelleted by ultracentrifugation. Cosedimentation of the various proteins with F-actin was analyzed by CBB staining of the gel. (D) Direct plot of binding of GST-CT2 to F-actin. A fixed amount of GST-CT2 (1 μM) was mixed with various amounts of F-actin (0–2.5 μM), followed by ultracentrifugation. Amounts of the free and bound GST-CT2 were quantified, and the (Da) percentage of bound GST-CT2 was plotted against the concentration of F-actin, and the (Db) K_d value was calculated by Scatchard analysis. (E) (Ea) Summary of the localization and functions of Girdin domains. (Eb) The proposed structure of Girdin.

CT1) and the C-terminal half (GFP-CT2) of the CT domain, and we examined their intracellular localization (Figure 3Ba). When expressed in Vero cells, the GFP-NT, GFP-M1, and GFP-M2 localized in the cytoplasm (Figures 3Bb–3Bd). The GFP-CT1 localized in both the nucleus and the plasma membrane, as shown by its colocalization with CM-Dil, a carbocyanine membrane probe (Figure 3Be), while GFP-CT2 apparently localized on the stress fibers (Figure 3Bf). These findings suggest that Girdin localizes on the actin filament via its CT2

domain, whereas it also associates with the plasma membrane via its CT1 domain. The nuclear localization of the GFP-CT1 seen here may be an artifact, because no accumulation of endogenous Girdin was visible in the nucleus (Figure 3A).

We next investigated the actin binding properties of the CT2 domain by actin cosedimentation assays (Figures 3C and 3D). The purified glutathione S-transferase (GST)-fused CT2 (GST-CT2) cosedimented with purified F-actin, as did α -actinin, whereas GST alone did not

(Figure 3C), indicating that GST-CT2 directly binds to F-actin. As the amount of F-actin increased, the binding of GST-CT2 with F-actin was saturated (Figure 3Da). The estimated dissociation constant (K_d) for F-actin was 1.03 μ M, indicating that Girdin has relatively low affinity for F-actin (Figure 3Db).

The domains of Girdin, their predicted functions, and the speculated structure of Girdin are summarized and illustrated in Figure 3E. Together, these findings allow us to propose that Girdin may possess an actin cross-linking property.

Girdin Is Required for the Formation of Actin Stress Fibers and Cell Migration

To assess the function of Girdin, we employed RNA-mediated interference (RNAi) to suppress (knockdown) the expression of Girdin in Vero cells. We introduced several Girdin small (21 nucleotide) interfering RNAs (Girdin siRNA) and a 21 nucleotide irrelevant RNAs (control siRNA) into Vero cells. Western blot analyses showed that transfection with the Girdin siRNAs effectively reduced the expression levels of Girdin by over 90% without affecting those of Akt and actin (Figure 4A). In order to verify the specificity of the knockdown experiments, the two oligonucleotides, Girdin siRNAs A and B, were utilized for Western blot analyses and other functional assays described in this study.

To test whether Girdin functions to promote the crosslinking of actin filaments, we examined the effects of Girdin knockdown on the organization of the actin cytoskeleton. Immunofluorescent staining with anti-Girdin Ab showed that the expression of Girdin was very low in the Girdin siRNA-transfected cells (Figure 4Bb). Staining of F-actin-rich structures with phalloidin revealed that the stress fibers were disrupted in the Girdin siRNA-transfected cells (Figure 4Bb), indicating that Girdin is essential for the formation of the stress fibers. When observed under higher magnification, Girdin siRNA-transfected cells contained markedly reduced thin and short stress fibers. Moreover, they lost their shape and formed with rugged boundaries that gave rise to the formation of multiple protrusions (leading edge) (Figure 4Bb, lower panel, and Figure 4C).

To further clarify the roles of Girdin in actin dynamics, we observed the behavior of the Girdin-depleted cells during migration in *in vitro* wound-healing assays (Figure 4D and Movies S1 and S2). We found that the Girdin siRNA-transfected cells facing the wound failed to produce extended lamellipodia at the leading edge and showed a migration defect that included multiple protrusions that were repeatedly stretched and shortened (Figure 4Db and Movie S2). These results suggest that Girdin is essential for organization of actin filaments during cell migration.

To test the specificity of the effect of the Girdin knockdown, we also introduced the Girdin siRNA into another cell line, SK-N-MC neuroblastoma cells, which stably express the RET receptor tyrosine kinase (Takahashi, 2001). Girdin siRNA-transfected SK-N-MC (RET) cells exhibited disruption of the stress fibers and limited formation of lamellipodia in response to the RET ligand, glial cell line-derived neurotrophic factor (GDNF) (Figure S3).

Localization of Girdin on Actin Filaments and Ultrastructure of the Girdin-Depleted Cells by Electron Microscopy

To further confirm the direct interaction of Girdin with actin filaments *in vivo* and its roles in actin organization, ultrastructural analysis was performed by deep-etch electron microscopy of "unroofed" Vero cells (Figure 5). Immunogold labeling revealed that Girdin molecules localize with actin filaments (Figure 5A). Higher-magnification views showed extensive colocalization of Girdin with the junctions between the actin filaments (Figure 5B).

Consistent with the immunofluorescence analysis, the density of the cortical actin filaments visible in electron micrographs of the cytoplasmic surface under the plasma membrane of Girdin-depleted Vero cells is lower than that in the control cells, where more tightly organized actin fibers predominate (Figure 5C). In the control siRNA-transfected cells, the filaments abut one another, run together without separating, and form thick cables tightly crosslinked by many molecules. Some filaments were oriented perpendicular to the other actin cables, resulting in interwoven and dense actin networks. In the Girdin siRNA-transfected cells, however, the actin bundles are sparse, and each actin filament is separated from another and is sometimes disrupted en route.

Phosphorylated Girdin Localizes to the Leading Edge of Migrating Cells

To gain insight into the role of Girdin phosphorylation by Akt, we examined the location of phosphorylated Girdin in Vero cells by staining with the anti-P-Girdin Ab (Figure 6A). In serum-starved quiescent cells, phosphorylation of Girdin was hardly detected throughout the cells (Figure 6A, top panel), consistent with the results of Western blot analyses (Figure 2D). When cells were stimulated with EGF (50 ng/ml), the immunostaining showed that phosphorylated Girdin appeared in the lamellipodia at the leading edge of migrating cells (Figure 6A, middle panel). The phosphorylated Girdin was also colocalized with Cortactin that exists at the leading edge (Figure 6B). Moreover, we observed that the stimulation of Vero cells with EGF enhanced the specific accumulation and localization of active Akt with phosphorylated Girdin in lamellipodia at the leading edge (Figure S4). In the Girdin siRNA-transfected cells, stimulation by EGF induced multiple leading edges. At these leading edges, the signals of phosphorylated Girdin were abolished as expected (Figure 6A, bottom panel), further supporting the specificity of the immunostaining. The nuclear signal seen in the immunostaining was still visible in the Girdin siRNA-transfected cells (Figure 6A, bottom panel), indicating that it was an artifact.

Akt Regulates the Association of Girdin with the Plasma Membrane

What is the mechanism that determines localization differences between the phosphorylated and nonphosphorylated forms of Girdin? Because the CT1 domain of Girdin localizes to the plasma membrane and contains the phosphorylation site, we hypothesized that it is the association of Girdin with the plasma membrane

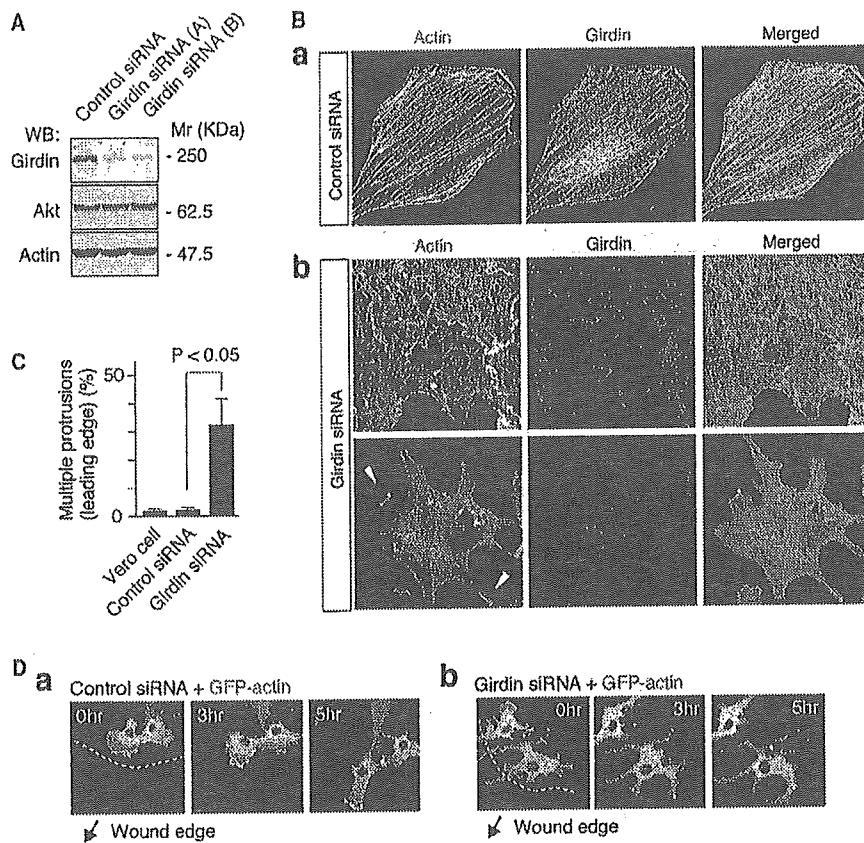


Figure 4. Girdin Is Essential for the Formation of Stress Fibers and Cell Migration

(A) Depletion of Girdin in Vero cells by siRNA. Total cell extracts from control siRNA- and Girdin siRNA-transfected Vero cells were subjected to Western blot analyses with anti-Girdin, anti-Akt, and anti-actin antibodies.
 (B) Vero cells were transfected with (Ba) control or (Bb) Girdin siRNAs and fixed 72 hr after transfection, followed by staining with Alexa488-phalloidin and anti-Girdin antibody. Arrowheads denote lamellipodia at the tips of protrusions.
 (C) After transfection of each siRNA, the number of cells with multiple protrusions was counted by staining with anti-Girdin antibody and Alexa488-phalloidin. More than 100 transfected cells were counted in each group. The results represent the means \pm SE.
 (D) Vero cells were cotransfected with GFP-actin and either (Da) control or (Db) Girdin siRNA and incubated for 48 hr. Cells were plated on fibronectin-coated glass coverslips and wounded to induce cell migration. Images were collected every 90 s for a period of 5–6 hr starting 2 hr after scraping. The arrows indicate the direction of cell migration into the wounds.

that is regulated by the phosphorylation. We found that a positively charged sequence of 19 amino acid residues (Arg-1389 to Lys-1407) upstream of the phosphorylation site (Figure 6Ca) resembles a consensus sequence for phosphatidylinositol 4,5-bisphosphate (PI[4,5]P₂) binding (Sechi and Wehland, 2000). When the GFP-CT1 in which the phosphoinositide binding site was deleted (termed GFP-CT1 Δ PB) was transfected into Vero cells, localization of GFP-CT1 Δ PB to the plasma membrane was not observed (Figure 6Cb). This finding suggested that the CT1 domain is anchored at the plasma membrane through binding to phosphoinositides.

To examine the phosphoinositide binding properties of Girdin, we performed a protein-lipid binding assay with purified GST fusion proteins containing the phosphoinositide binding site of Girdin (Figures 6D and 6E). In the experiment, we utilized the CT domain fused with

GST instead of the CT1 domain (Figure 6Da), because the GST-CT1 fusion protein was easily degraded during expression and purification procedures. As shown in Figure 6Ea, GST-CT bound selectively to PI(4)P and weakly to PI(3)P, but to none of the other phosphoinositides or phospholipids. The binding property of GST-CT to PI(4)P and PI(3)P was abrogated when the phosphoinositide binding site was deleted (Figure 6Eb). We also found that mutants of the CT1 domain, in which the positively charged basic residues were replaced with alanines (Girdin PBala mutant), failed to bind to the phosphoinositides and were delocalized from the plasma membrane (Figure S5), suggesting that the positive electrostatic charge generated by the basic residues in the phosphoinositide binding motif is required for the association of Girdin with the plasma membrane.

Since the phosphoinositide binding site is located near the Akt phosphorylation site (Figure 6Ca), the sup-

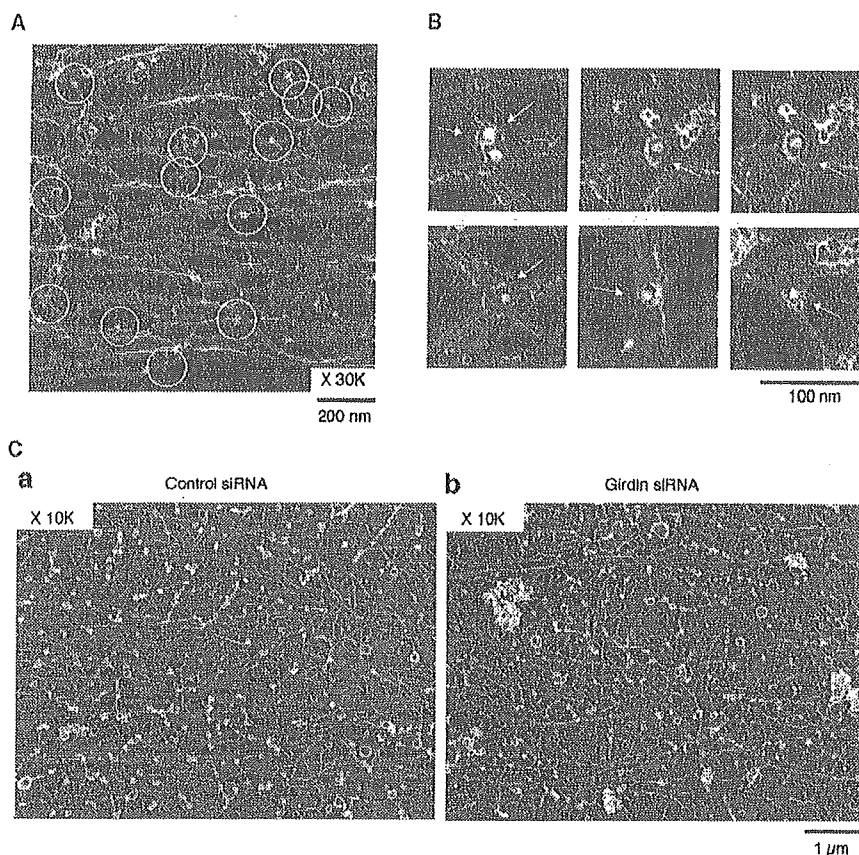


Figure 5. Electron Microscopic Analysis of Girdin Localization and the Effect of Its Depletion on Actin Organization

(A) Immunogold electron microscopy with anti-Girdin antibody.

(B) Circles indicate the immunogold signals of Girdin molecules, shown here under higher magnification. Arrows denote the immunogold signals.

(C) Ultrastructure of actin filaments in Vero cells transfected with either (Ca) control or (Cb) Girdin siRNA.

position was made that Akt might control the localization of Girdin by regulation of its phosphoinositide binding property. To determine if this is the case, we examined the phosphoinositide binding property of phosphorylated GST-CT. Purified GST-CT was effectively phosphorylated by Akt *in vitro* (Figure 6Db). GST-CT was then subjected to the protein-lipid binding assay, in which binding was detected by anti-P-Girdin Ab. As shown in Figure 6Ec, the phosphorylated GST-CT bound to neither PI(4)P nor PI(3)P. In addition, actin cosedimentation assays showed that the phosphorylation of GST-CT did not attenuate its affinity for F-actin (Figure 6F), and that the binding kinetics was similar to that of GST-CT2 (Figure 3D). These findings suggested that the binding of Girdin to the phosphoinositides, but not to F-actin, is attenuated by phosphorylation.

Moreover, we investigate whether the membrane association of Girdin is regulated by EGF treatment, by using COS7 cells expressing either the GFP-full-length Girdin WT or SA mutant. The results supported the view that phosphorylation at Ser-1416 by Akt is necessary

for the delocalization of Girdin from the plasma membrane. (Figure S6).

Phosphorylation of Girdin by Akt Is Required for Cell Migration

The localization of phosphorylated Girdin at the leading edge prompted us to test whether the phosphorylation of Girdin is involved in cell motility. After wounding a confluent monolayer of Vero cells, immunostaining with anti-P-Girdin Ab showed that the level of Girdin phosphorylation in cells at the wound edge increased soon after scratching, reached a maximum at 8 hr, and lasted for at least 12 hr (Figure 7A). The implication is that the phosphorylation of Girdin may play an important role in cell motility. Thus, the role of Girdin in cell motility was examined with Boyden chamber assays. The Girdin knockdown significantly retarded the ability of Vero cells to migrate in response to EGF (50 ng/ml) added to the lower chamber (Figure 7B). We also found that expression of the CT domain in Vero cells significantly attenuated cell migration (Figure 7B), supporting the

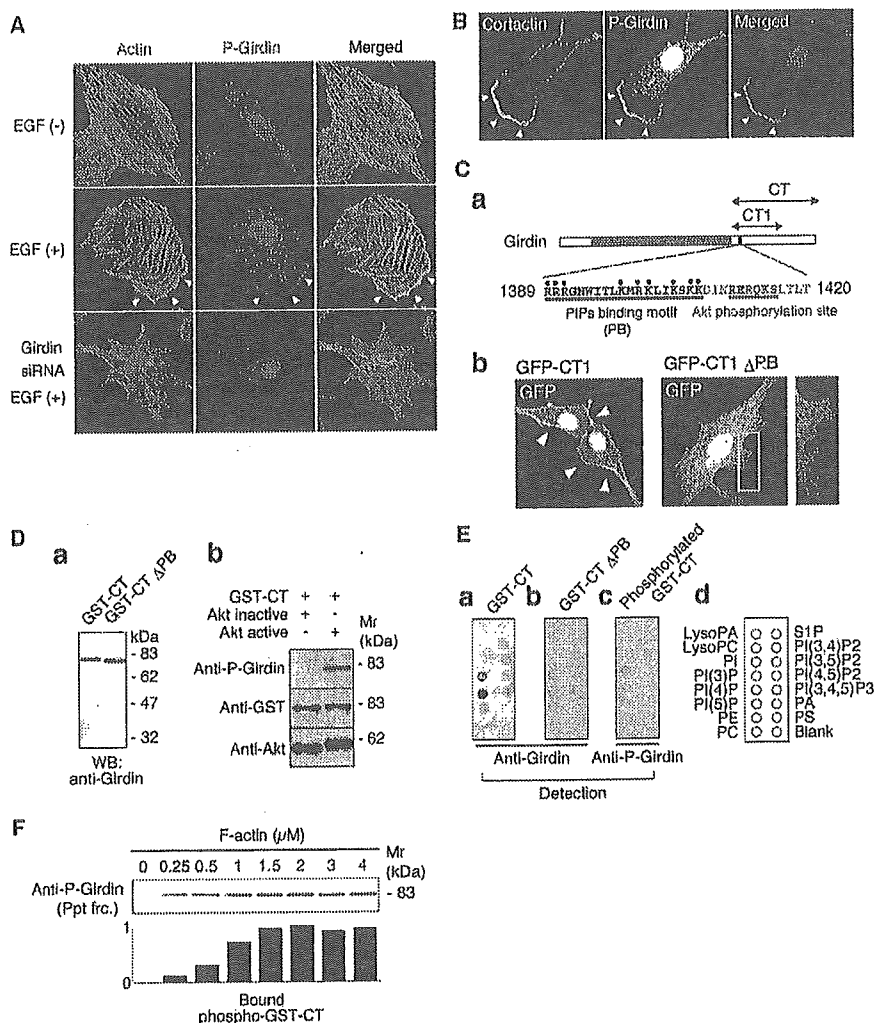


Figure 6. Effects of Girdin Phosphorylation on Its Localization and Interaction with Phosphoinositides

(A) Quiescent (upper panel), EGF (50 ng/ml)-stimulated (middle panel), and Girdin siRNA-transfected (lower panel) Vero cells were fixed and stained with Alexa488-phalloidin and anti-phospho Girdin (P-Girdin) antibody. Arrows denote the lamellipodia where the phosphorylated Girdin accumulates.

(B) Migrating Vero cells were stained with anti-Cortactin and anti-P-Girdin antibody.

(C) (Ca) The putative phosphoinositide binding site (PB) upstream of the Akt phosphorylation site in Girdin is indicated. (Cb) Vero cells were transfected with either GFP-CT1 (left) or GFP-CT1 in which the phosphoinositide binding site was deleted (GFP-CT1 ΔPB) (right). Arrows denote GFP signals at the plasma membrane.

(D) Purification of GST-CT and protein-lipid overlay assays. (Da) Purified GST-CT and GST-CT ΔPB were analyzed by Western blotting with anti-Girdin antibody. (Db) Phosphorylation of purified GST-CT by recombinant Akt in vitro. The phosphorylated GST-CT in an in vitro kinase assay was detected with anti-P-Girdin antibody.

(E) Protein-lipid overlay assays with (Ea) GST-CT, (Eb) GST-CT ΔPB, and the (Ec) phosphorylated GST-CT. The lipid binding of both GST-CT and GST-CT ΔPB was detected with anti-Girdin antibody, whereas that of phosphorylated GST-CT was detected with anti-P-Girdin antibody.

(Ed) The various lipids spotted on the membrane (100 pmol lipid per spot) are indicated. PA, phosphatidic acid; PC, phosphocholine; PI, phosphatidylinositol; PE, phosphatidylethanolamine; PS, phosphatidylserine; S1P, sphingosine-1-phosphate.

(F) Binding of phosphorylated Girdin CT to F-actin. GST-CT was phosphorylated by Akt in vitro (Db) and subjected to an actin cosedimentation assay. A fixed amount of GST-CT (1 μM) was phosphorylated in vitro and mixed with various amount of F-actin (0–4 μM), followed by ultracentrifugation. The amount of phosphorylated GST-CT bound to F-actin in the pellet fraction (Ppt frac.) was monitored by Western blot analyses with anti-P-Girdin antibody.

notion that the interaction of endogenous Girdin with actin filaments is important for integral cell migration. Consistent with previous studies (Higuchi et al., 2001; Kim et al., 2001), the depletion of Akt by siRNA also

attenuated the migration (Figure 7B), which suggests that intrinsic Akt activity is requisite for Vero cells to migrate through the pores in this assay system.

To next examine whether adding Girdin exogenously

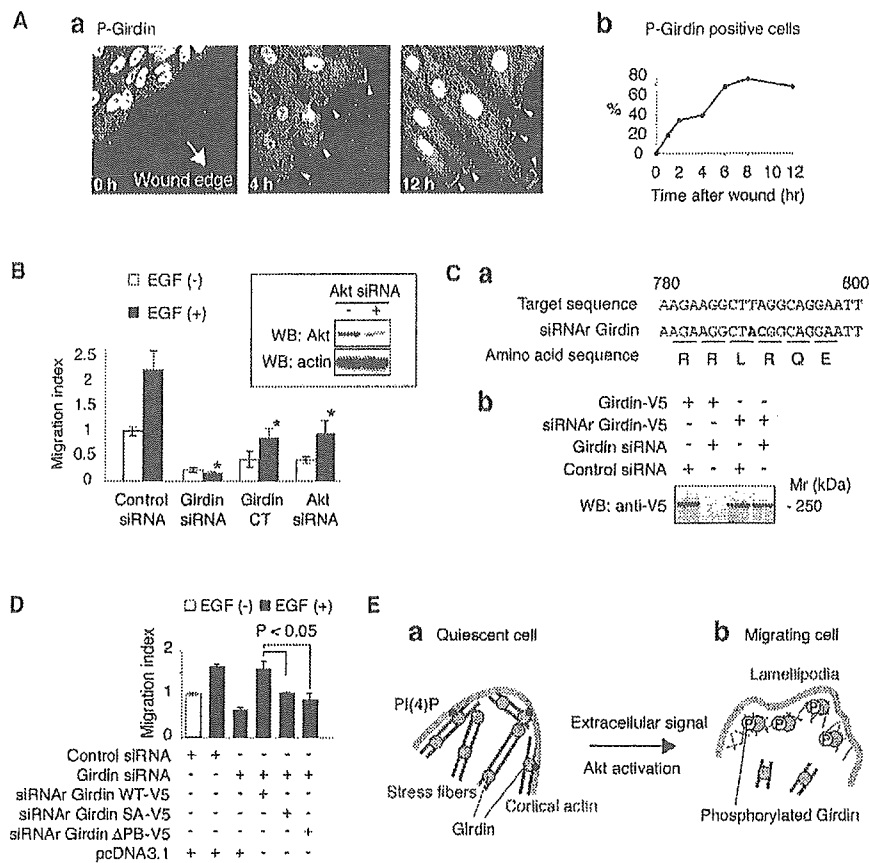


Figure 7. Phosphorylation of Girdin Regulates Cell Migration

(A) Girdin is phosphorylated at the leading edge during cell migration. (Aa) After scratching a monolayer of Vero cells, the cells facing the wound were fixed and stained with anti-P-Girdin antibody. Arrowheads denote the signals of the phosphorylated Girdin. (Ab) The phosphorylation of Girdin localizing at the leading edge increases in a time-dependent fashion.

(B) Vero cells were transfected with GFP (0.5 μ g) and either siRNA (20 pmol) or Girdin CT (2.5 μ g), incubated for 48 hr, and subjected to Boyden chamber assays in the presence or absence of EGF (100 ng/ml) in the lower chamber. Asterisks indicate statistical significance (Student's *t* test; **p* < 0.05) compared with control. The inset shows the depletion of Akt in Vero cells by siRNA. The results represent the mean \pm SE.

(C) Generation of an siRNA-resistant (siRNAr) mutant of Girdin. (Ca) The target sequence of Girdin siRNA ("B" in Figure 4A) and the nucleotide substitution for the generation of the siRNAr version are indicated. (Cb) Cell lysates from COS7 cells cotransfected with indicated siRNAs and constructs were analyzed by Western blotting with anti-V5 antibody.

(D) Vero cells were cotransfected with GFP (0.5 μ g), siRNAs (20 pmol), and indicated constructs (2.5 μ g), incubated for 48 hr, and subjected to Boyden chamber assays. Expression levels of Girdin mutants in cells prior to plating for migration assays were monitored by Western blot analysis with anti-V5 antibody and were found to be similar (data not shown). The results represent the mean \pm SE.

(E) A proposed model for the regulation of cell motility by the phosphorylation of Girdin. In (Ea) quiescent cells, Girdin crosslinks actin filaments and anchors cortical actin at the plasma membrane, whereas during (Eb) cell migration, Akt-mediated phosphorylation allows Girdin to localize at the leading edge and contribute to the formation of short-branched filaments in the lamellipodium.

restores the defect in cell migration observed in the knockdown cells, we constructed siRNA-resistant (siRNAr) versions of Girdin harboring silent mutations (Figure 7C). As shown in Figure 7D, the expression of the siRNAr-Girdin WT fully restored migratory response to EGF. In contrast, the expression of the siRNAr-Girdin mutants in which the Ser-1416 was mutated to Ala (siRNAr-Girdin SA), the phosphoinositide binding site was deleted (siRNAr-Girdin Δ PB), or the basic residues in the phosphoinositide binding site were replaced with alanines (siRNAr-Girdin PBala) failed to complement the migration defect (Figure 7D and Figure S5C). We

also confirmed these findings by performing migration assays with a human fibrosarcoma cell line, HT-1080 (Figure S7).

Finally, we directly examined the movement of Vero cells expressing the Girdin mutants by wound-healing assays (Figure S8 and Movies S3–S6). Cells expressing Girdin WT effectively and rapidly moved into the wound (Movie S3), but those expressing Girdin SA exhibited elongated shape. Moreover, the location of the nuclei of the latter cells seemed to be fixed and motionless, suggesting that the cells could not undergo detachment from the matrix (Movie S4). Cells expressing Gir-

din Δ PB and Girdin PBala were less locomotive compared with those expressing Girdin WT (Movies S5 and S6, respectively). These results demonstrate that expression of the Girdin mutants impairs proper directional cell migration. Considered with the findings shown in Figure 6 and Figure S6, these data indicate that the regulation of an interaction between Girdin and the plasma membrane by Akt is crucial for cell migration.

Discussion

The Structure of Girdin/APE and Its Roles in Actin Organization

In a search for molecules that interact with Akt, we have identified a novel, to our knowledge, actin binding protein, designated Girdin/APE, that is essential for actin organization. Four different regions can be distinguished in the Girdin molecule based on the sequences of its subunits, subcellular localization, and functions: an N-terminal region that seems to facilitate the formation of a dimer (NT), an extremely long coiled-coil region, a region that binds to the plasma membrane through the interaction with phosphoinositides (CT1), and a C-terminal region that encompasses an actin binding site (CT2). The amino acid sequence of the CT2 domain shows no homology with the calponin homology (CH) domain, a common actin binding domain that is present in most actin binding proteins such as α -actinin, filamins, fimbrin, spectrins, cortexillins, and dystrophin (Gimona et al., 2002), suggesting that Girdin represents a novel class of actin binding proteins.

Analysis of the sequence of Girdin reveals that it includes 135 heptad repeats, $(abcdefg)_{135}$, between Leu-253 and Lys-1375 that correspond to a central rod domain. Within the repeats, positions *a* and *d* are preferentially occupied by hydrophobic residues like Leu, Ile, Met, or Val (Figure S1), which is consistent with the signature of canonical coiled-coil structures that wind around each other in a superhelix (Cohen and Parry, 1994). The oligomerization properties of coiled-coil sequences are determined by the distribution of β -branched residues in the *a* or *d* positions (Harbury et al., 1993; Faix et al., 1996). Val and Ile in *a* favor dimerization, they favor tetramerization in *d*, and their presence in both *a* and *d* facilitates the formation of trimers. In the coiled-coil sequence of Girdin, 22 repeats have Val or Ile in the *a* position, whereas they are present in the *d* position of only 9 repeats, suggesting that the coiled-coil domain of Girdin tends to form a dimer. This is consistent with our findings suggested by gel filtration that the NT domain of Girdin forms a dimer (Figure S2).

It has been established that the possession of two actin binding sites enables crosslinking or bundling proteins to link filaments and to stabilize higher-order assemblies of actin filaments (Pollard, 2002). Possessing two actin binding CT2 domains in juxtaposition, the dimeric Girdin molecules seem to be designed to gather actin filaments together into bundles or a meshwork. Consistent with this possibility are the findings of immunofluorescent staining and electron microscopy that the depletion of Girdin interfered with actin networks, leading to the disruption of stress fibers, cortical

actin filaments, and actin meshwork at the leading edge. During migration, the Girdin knockdown cells produced multiple protrusions, resulting in limited directional migration. These observations indicate that Girdin fulfills an essential function in determining the stability and integrity of actin bundles and meshwork that mediates a variety of important biological processes. Eukaryotic cells have a fail-safe mechanism in the multiple actin crosslinking proteins that share overlapping functions (Pollard, 2002). The phenotypic consequences of the depletion of Girdin indicate that the presence of other proteins cannot completely compensate for its loss. Because the speculated primary structure, molecular size, and putative function of Girdin are reminiscent of those of filamin (Stossel et al., 2001), it is important to clarify the functional difference and synergism between the two.

We found that the CT1 domain of Girdin associates with the plasma membrane through the cluster of basic amino acid residues Arg-1389 to Lys-1407. This positively charged sequence is related to a consensus sequence for PI(4,5)P₂ binding, which has been found in gelsolin, villin, profilin, vinculin, and other various cytoskeletal proteins (Janmey et al., 1992). Unexpectedly, our experiment showed that the basic amino acid cluster in Girdin does not bind to PI(4,5)P₂, but binds to PI(4)P and binds weakly to PI(3)P. Considering that PI(4)P, but not PI(3)P, is abundant in mammalian cells (Vanhaesebroeck et al., 2001), it is plausible to conclude that Girdin binds to PI(4)P, which resides in the membranes of mammalian cells in an amount equal to that of PI(4,5)P₂. We speculate that it stabilizes the cortical actin filaments by anchoring them at the plasma membrane.

Roles of Girdin and Its Regulation in Cell Motility

Relatively little is known about how cells regulate actin crosslinking proteins in response to external stimuli (Pollard, 2002; Small et al., 2002). In the present study, we found that Akt phosphorylates Girdin *in vitro* and in intact cells. The phosphorylation of Girdin was induced by EGF and during cell migration, suggesting a significance for phosphorylation in physiological cellular events. In migrating Vero fibroblasts, the phosphorylated Girdin preferentially localizes to lamellipodia at the leading edge, which is in line with our and previous observations that activated Akt is also localized at the leading edge during migration in mammalian cells (Higuchi et al., 2001; Kim et al., 2001; Figure S4). It is plausible that Akt, activated downstream of PI3K, translocates from the cytosol to the leading edge through its PH domain, and subsequently phosphorylates Girdin on the actin filaments at the front of the cells.

How does Akt regulate the function of Girdin by phosphorylation? Insight into this issue comes from our observation that the phosphorylation of the CT domain of Girdin affects *in vitro* binding to PI(4)P. Because the phosphorylation site is present in the neighborhood of the phosphoinositide binding site, it is speculated that phosphorylation induces a conformational change around these sites, and this change in turn alters affinity for the phosphoinositide. We further found that the phosphorylated CT domain retains the property of actin

binding, and its affinity for F-actin is comparable to that of the nonphosphorylated form. Based on these observations, we speculate that phosphorylation by Akt releases Girdin from PI(4)P and allows it to localize at the leading edge in order to crosslink the newly generated actin filaments in the lamellipodium network, as illustrated in Figure 7E.

The leading lamellipodium of motile cells is a sheet-like protrusion filled with actin filaments at high density (Small et al., 2002). Because long and flexible actin filaments cannot sustain a pushing force (Pollard and Borisy, 2003), cells must create a dense array of short-branched filaments by utilizing crosslinking proteins, which allow nascent filaments to push against the membrane at the leading edge. The major crosslinking components at lamellipodium are filamin and α -actinin (Small et al., 2002). Cells derived from human malignant melanomas lacking filamin had unstable lamellipodia and exhibited impaired locomotion (Stosself et al., 2001). *Dictyostelium* cells lacking both α -actinin and ABP-120 (the filamin homolog) showed motility defects (Rivero et al., 1996). Both of these proteins have a relatively low affinity for actin filaments, with K_d values in the micromolar range. This low affinity enables their rapid binding and dissociation with the filaments and allows networks of actin filaments to passively change shape when prolonged force is applied while resisting rapid deformations (Pollard, 2002). This is also the case with Girdin, which has a low affinity for F-actin, with a K_d value of $\sim 1 \mu\text{M}$. An important goal is to reveal functional divergence and structural complementation between Girdin and other crosslinking proteins in the lamellipodium.

The role of Girdin in cell migration is supported by the findings that Girdin knockdown cells migrated poorly and exhibited insufficient lamellipodium formation at their leading edge. However, they revert to normal behavior when siRNA-Girdin is added. In contrast, cells expressing siRNA-Girdin SA, ΔPB , and PBala mutants exhibited limited migration (Figure 7, Figure S8, and Movies S3–S6). As Girdin SA may be constantly anchored at the plasma membrane without undergoing phosphorylation, and Girdin ΔPB and PBala do not associate with the plasma membrane (Figure S6), our findings suggest that spatially selective regulation of Girdin phosphorylation by Akt at the cytoplasm-membrane interface is essential for reorganization of the actin cytoskeleton.

Activation of Akt is correlated with an increase in cell migration and invasion in several mammalian systems. The overexpression of active Akt promotes cell motility in mammalian cells such as fibroblasts, fibrosarcoma cells, and vascular endothelial cells (Higuchi et al., 2001; Kim et al., 2001; Morales-Ruiz et al., 2000). Rac and Cdc42, small GTPases essential for lamellipodia formation and establishment of cell polarity, activate Akt at the leading edge of fibroblasts (Higuchi et al., 2001). Akt is involved in the trafficking and recycling of vitronectin and fibronectin receptors ($\alpha\text{v}\beta 3$ and $\alpha 5\beta 1$ integrins, respectively), which regulate cell spreading and migration (Roberts et al., 2004). Finally, the association of Pak1 (p21-activated protein kinase) with Nck, an adaptor protein, is crucial for cell movement and is modulated by Akt (Zhou et al., 2003). Along with our

present findings, these data indicate the involvement of Akt in cell motility. In addition, it was recently demonstrated that Akt and its substrate glycogen synthase kinase-3 β (GSK-3 β) are essential proteins in the determination of axon-dendrite polarity of neurons (Yoshimura et al., 2005; Jiang et al., 2005). Because the depletion of Girdin results in the formation of multiple leading edges and limited directional migration in Vero fibroblasts, the possible involvement of the Akt-Girdin pathway in the regulation of cell polarity should not be overlooked.

In conclusion, we demonstrated a novel, to our knowledge, role of Girdin/APE in actin organization and cell motility that is regulated by Akt. Anai et al. (2005) reported that Girdin/APE also functions as an enhancer of Akt and stimulates DNA synthesis. When Girdin/APE and Akt were overexpressed in cells, they found that cell proliferation was inhibited and apoptosis was induced. Thus, further investigation could shed light on important roles of Girdin/APE in different cellular processes.

Experimental Procedures

Yeast Two-Hybrid Assays

To identify proteins interacting with Akt, a full-length cDNA encoding human Akt1 was inserted into the pAS2 vector (Clontech). The resulting construct was used as bait to screen a human fetal brain MATCHMAKER cDNA library as previously described (Murakami et al., 2002). Two positive plasmids containing cDNA inserts were selected and sequenced. They contained the cDNA fragments encoding the C-terminal region of Girdin (residues 1217–1870). A full-length cDNA encoding Girdin was isolated from the human fetal brain poly A⁺ RNA by 5' rapid amplification of cDNA ends (5'-RACE system, Invitrogen). Additionally, we performed yeast two-hybrid binding assays with purified pAS and pACT constructs containing the fragments of human Akt1 and Girdin cDNAs.

Plasmids

Wild-type, constitutively active, and dominant-negative human Akt1 constructs were generously provided by Y. Gotoh (University of Tokyo). The constructs of pcDNA3.1-, pGEX-, and pEGFP-Girdin fragments were produced as described elsewhere (Murakami et al., 2002). EGFP was fused to the amino termini, and V5 and myc tags were fused to the carboxyl termini of the proteins. Girdin mutants were generated by using the QuikChange site-directed mutagenesis kit (Stratagene) according to the manufacturer's protocol. The siRNA-resistant Girdin was created by introducing two silent mutations into Girdin at nucleotides 780–800 (5'-AAGAAAGCTACGG CAGGAATT-3') (underline indicates mutations).

Antibodies

Rabbit anti-Girdin polyclonal antibody was developed against the 19 carboxyl-terminal amino acids of Girdin and affinity-purified with the immunized peptide. The anti-phospho Girdin polyclonal antibody was supplied by Kumamoto Immunochemical Laboratory, Transgenic, Inc. (Kumamoto, Japan). It was raised by immunizing rabbits with a keyhole limpet hemocyanin-conjugated phosphopeptide corresponding to Girdin amino acid sequence 1408–1420 (CDINRERQKpSLTLT). Antiserum was purified as a bound fraction of the phosphopeptide-conjugated column.

Other antibodies used in this study include anti-Akt polyclonal antibody (Cell Signaling Technology), anti-phospho Akt polyclonal antibody (Cell Signaling Technology), and anti-Cortactin monoclonal antibody (Upstate).

Kinase Assays

Immunoprecipitates with anti-V5 antibody (Invitrogen) from COS7 cells expressing Girdin CT-V5 WT or SA or purified GST-CT were incubated with recombinant active or inactive Akt (500 ng) (Up-

state) with 10 μCi [γ - ^{32}P]ATP (3000 Ci/mmol, Amersham) in kinase buffer (20 mM MOPS, 25 mM β -glycerophosphate, 5 mM EGTA, 15 mM MgCl_2 , 1 mM dithiothreitol, and 1 mM NaVO_3). Mixtures were incubated at 30°C for 30 min, and reactions were terminated by the addition of Laemmli sodium dodecyl sulfate (SDS) sample dilution buffer (20 mM Tris-HCl [pH 6.8], 2 mM EDTA, 2% SDS, 10% sucrose, 20 $\mu\text{g}/\text{ml}$ bromophenol blue, 80 mM dithiothreitol).

Immunofluorescent Staining

Vero cells were plated on fibronectin- (10 $\mu\text{g}/\text{ml}$, Sigma) and collagen I (10 $\mu\text{g}/\text{ml}$, Upstate)-coated coverslips or glass base dishes, fixed, and stained with the indicated antibodies. Fluorescence was examined by using a confocal laser-scanning microscope (Fluoview FV500, Olympus).

Actin Cosedimentation Assays

F-actin cosedimentation assays were performed according to the manufacturer's protocol (Cytoskeleton). Briefly, purified GST fusion proteins, GST alone, and α -actinin (Cytoskeleton) were incubated for 30 min at room temperature with 40 μg pure actin filaments. The final concentration of F-actin was 18 μM . Filaments were subsequently pelleted by centrifugation (100,000 \times g) (Beckman). The cosedimented proteins were resolved by SDS-PAGE and detected by either Coomassie Brilliant Blue (CBB) staining or Western blot analyses with anti-GST antibody (Cell Signaling Technology) or anti-phospho Girdin Ab.

For quantitative analyses, a fixed concentration of GST-Girdin CT2 (1 μM) was mixed with increasing amounts of F-actin (0–2.5 μM) in polymerization buffer and incubated at room temperature for 30 min. Proteins were centrifuged as described above, and total pellets and supernatants were loaded separately on SDS-PAGE. Protein bands were detected by CBB staining and scanned and quantified with the software program WinROOF (Mitani Corp., Fukui, Japan).

RNA Interference

The siRNA-mediated knockdown of Girdin and Akt was performed by using previously described methods (Watanabe et al., 2004). The targeted sequences that effectively mediated the silencing of the expression of Girdin are as follows (only sense sequences are shown): 5'-AACCAGGTCATGCTCCAAATT-3' (nucleotides 145–165, Girdin siRNA [A]) and 5'-AAGAAGGCTTAGGCAGGAATT-3' (nucleotides 780–800, Girdin siRNA [B]). The 21 nucleotide synthetic duplexes were prepared by Qiagen. The siRNA specific to human Akt1 was purchased from Qiagen. Vero cells were transfected with the siRNAs or a 21 nucleotide irrelevant RNA (Qiagen) as a control, by using lipofectamine 2000 (Invitrogen) according to the manufacturer's protocol.

Freeze-Replica Electron Microscopy of the Cytoplasmic Cell Surface

Electron microscopy of the cytoplasmic surface of the cell membrane was carried out according to previously described methods (Heuser, 1989, 2000; Usukura, 1993). Vero cells cultured on glass coverslips (3 mm in diameter, standard #1 Matsunami, Osaka, Japan) were transfected with siRNAs. Immediately after being unroofed from the apical cell membrane, the cells were fixed for 30 min in 2.5% glutaraldehyde in buffer A (70 mM KCl, 5 mM MgCl_2 , 3 mM EGTA, 30 mM HEPES buffer adjusted at pH 7.4 with KOH). After being washed with buffer A/distilled water, specimens were quickly frozen with liquid helium by using the rapid-freezing device (Eiko, Tokyo, Japan). Samples were then freeze etched and rotary shadowed with platinum-carbon, in a newly developed freeze etching device (FR9000, HITACHI, Ibaraki, Japan). For immunolabeling of Girdin molecules, the unroofed cells were fixed for 30 min in 4% paraformaldehyde/0.5% glutaraldehyde in buffer A. After being washed three times with buffer B (100 mM NaCl, 30 mM HEPES, 2 mM CaCl_2), the samples were quenched and blocked, and then labeled for 1 hr at 37°C with primary and secondary 10 nm gold-conjugated antibodies (Amersham) in buffer B containing 1% BSA. Finally, specimens were rapidly frozen and freeze etched as described above.

Scratch-Induced Cell Migration and Time-Lapse Imaging

Directional cell migration of Vero cells was stimulated in a monolayer by using an in vitro scratch wound assay (Watanabe et al., 2004). Vero cells were seeded on fibronectin-precoated coverslips or 35 mm glass base dishes and were transfected with indicated siRNAs. A total of 48 hr after the transfection, the confluent Vero cells were scratched with a 200 μl disposable plastic pipette tip and were allowed to migrate toward the wound. The cells were fixed at the indicated times for immunofluorescent staining. For time-lapse observation, cells were cotransfected with siRNAs and GFP-actin and were subjected to the scratch wound assays. The cells at the wound edges were observed with a confocal laser scanning microscope (Fluoview FV500, Olympus).

Three-Dimensional Cell Migration Assays

To assess the motility of cells transfected with various constructs or siRNAs, we performed the modified Boyden chamber migration assay, which enabled us to count GFP-labeled cells migrating across a fluorescence-blocking planar micropore membrane by using HTS FluoroBlok Insert (8.0 μm pores, 24-well format, Becton Dickinson). Both sides of the membrane were coated with 10 $\mu\text{g}/\text{ml}$ fibronectin for 12 hr at 37°C and were washed with phosphate-buffered saline (PBS). The chambers were then placed in 24-well dishes filled with Dulbecco's modified Eagle's medium (DMEM) containing 0.1% BSA with or without 20 ng/ml human recombinant EGF. For migration assays of HT-1080 cells, DMEM with 10% fetal bovine serum (FBS) was added to the lower chamber. Cells (1×10^5) were transfected with GFP (0.5 μg , to identify transfected cells), indicated constructs (2.5 μg), and siRNAs (20 pmol) in 24-well plates, plated in the upper compartment, and allowed to migrate through the pores of the membrane for 4 hr. Cell motility was quantified by using a fluorescence microscope to count the GFP-positive cells that had migrated through the membrane.

Protein-Lipid Overlay Assays

GST fusion proteins were expressed in DH5 α or BL21-CodonPlus (Stratagene) cells and purified by using conventional methods. Binding of the purified GST-CT to phospholipids was examined at 4°C by using a PIP-Strip (Echelon Bioscience) according to the manufacturer's protocol. Bound GST-CT proteins were detected with either anti-Girdin or anti-phospho Girdin antibodies.

Data Analysis

Data are presented as the mean \pm SE. Statistical significance was evaluated by Student's *t* test.

Supplemental Data

Supplemental Data including eight figures, six movies, and Supplemental Experimental Procedures are available at <http://www.developmentalcell.com/cgi/content/full/9/3/389/DC1/>.

Acknowledgments

We thank Y. Gotoh (University of Tokyo) for providing Akt cDNAs and helpful discussion, T. Fukuda (Tohoku University) for helpful discussion, M. Nakayama (Nagoya University) for discussions on migration assays, K. Kadomatsu and K. Ichihara (Nagoya University) for providing HT-1080 cells, and N. Saka and A. Muraki (Nagoya University) for help in characterization of Girdin. This work was supported by Grants-in-Aid for Center of Excellence (COE) Research, Scientific Research (A), and Scientific Research on Priority Area "Cancer" from the Ministry of Education, Culture, Sports, Science and Technology of Japan (to M.T.). A.E. is a fellow of the Japan Society for the Promotion of Science.

Received: February 16, 2005
Revised: May 19, 2005
Accepted: August 3, 2005
Published: September 6, 2005

References

Alessi, D.R., Caudwell, F.B., Andjelkovic, M., Hemmings, B.A., and Cohen, P. (1996). Molecular basis for the substrate specificity of

- protein kinase B; comparison with MAPKAP kinase-1 and p70 S6 kinase. *FEBS Lett.* 399, 333–338.
- Anai, M., Shojima, N., Katagiri, H., Ogihara, T., Sakoda, H., Onishi, Y., Ono, H., Fujishiro, M., Fukushima, Y., Horike, N., et al. (2005). A novel protein kinase B (PKB)/AKT-binding protein enhances PKB kinase activity and regulates DNA synthesis. *J. Biol. Chem.* 280, 18525–18535.
- Brazil, D.P., Park, J., and Hemmings, B.A. (2002). PKB binding proteins: getting in on the Akt. *Cell* 111, 293–303.
- Chung, Y., Potikyan, G., and Firtel, R.A. (2001). Control of cell polarity and chemotaxis by Akt/PKB and PI3 kinase through the regulation of PAKs. *Mol. Cell* 7, 937–947.
- Cohen, C., and Parry, D.A.D. (1994). α -helical coiled-coils: more facts and better prediction. *Science* 265, 488–489.
- Datta, S.R., Brunet, A., and Greenberg, M.E. (1999). Cellular survival: a play in three Akts. *Genes Dev.* 13, 2905–2927.
- Etienne-Manneville, S., and Hall, A. (2002). Rho GTPases in cell biology. *Nature* 420, 629–635.
- Faix, J., Steinmetz, M., Boves, H., Kammerer, R.A., Lottspeich, F., Mintert, U., Murphy, J., Stock, A., Aebi, U., and Gerisch, G. (1996). Cortaxillins, major determinants of cell shape and size, are actin-binding proteins with a parallel coiled-coil tail. *Cell* 86, 631–642.
- Gimona, M., Djinic-Carugo, K., Kranewitter, W.J., and Winder, S.J. (2002). Functional plasticity of CH domains. *FEBS Lett.* 513, 98–106.
- Harbury, P.B., Zhang, T., Kim, P.S., and Alber, T. (1993). A switch between two, three and four stranded coiled-coils in GCN4 leucine zipper mutants. *Science* 262, 1401–1407.
- Heuser, J. (1989). Effect of cytoplasmic acidification on clathrin lattice morphology. *J. Cell Biol.* 108, 401–411.
- Heuser, J. (2000). The production of 'cell cortices' for light and electron microscopy. *Traffic* 1, 545–552.
- Higuchi, M., Masuyama, N., Fukui, Y., Suzuki, A., and Gotoh, Y. (2001). Akt mediates Rac/Cdc42-regulated cell motility in growth factor-stimulated cells and invasive PTEN knockout cells. *Curr. Biol.* 11, 1958–1962.
- Janmey, P.A., Lamb, J., Allen, P.G., and Matsudaira, P.T. (1992). Phosphoinositide-binding peptides derived from the sequence of gelsolin and villin. *J. Biol. Chem.* 267, 11818–11823.
- Jiang, H., Guo, W., Liang, X., and Rao, Y. (2005). Both the establishment and the maintenance of neuronal polarity require active mechanism: critical roles of GSK-3 β and its upstream regulation. *Cell* 120, 123–135.
- Kim, D., Kim, S., Koh, H., Yoon, S., Chung, A., Cho, K.S., and Chung, J. (2001). Akt/PKB promotes cancer cell invasion via increased motility and metalloproteinase production. *FASEB J.* 15, 1953–1962.
- Lauffenburger, D.A., and Horwitz, A.F. (1996). Cell migration: a physically integrated molecular process. *Cell* 84, 359–369.
- Lupas, A., Van Dyke, M., and Stock, J. (1991). Predicting coiled coils from protein sequence. *Science* 252, 1162–1164.
- Meili, R., Ellsworth, C., Lee, S., Reddy, T.B., Ma, H., and Firtel, R.A. (1999). Chemoattractant-mediated transient activation and membrane localization of Akt/PKB is required for efficient chemotaxis to camp in *Dictyostelium*. *EMBO J.* 18, 2092–2105.
- Merlot, S., and Firtel, R.A. (2003). Leading the way: directional sensing through phosphatidylinositol 3-kinase and other signalling pathways. *J. Cell Sci.* 116, 3471–3478.
- Morales-Ruiz, M., Fulton, D., Sowa, G., Languino, L.R., Fujio, Y., Walsh, K., and Sessa, W.C. (2000). Vascular endothelial growth factor-stimulated actin reorganization and migration of endothelial cells is regulated via the serine/threonine kinase Akt. *Circ. Res.* 86, 892–896.
- Murakami, H., Yamamura, Y., Shimono, Y., Kawai, K., Kurokawa, K., and Takahashi, M. (2002). Role of Dok1 in cell signaling mediated by Ret tyrosine kinase. *J. Biol. Chem.* 277, 32781–32790.
- Pollard, T.D. (2002). Actin and actin-binding proteins. In *Cell Biology*, T.D. Pollard and W.C. Earnshaw, eds. (New York: W.B. Saunders), pp. 557–577.
- Pollard, T.D., and Borisy, G.G. (2003). Cellular motility driven by assembly and disassembly of actin filaments. *Cell* 112, 453–465.
- Revenu, C., Athman, R., Robine, S., and Louvard, D. (2004). The co-workers of actin filaments: from cell structures to signals. *Nat. Rev. Mol. Cell Biol.* 5, 1–12.
- Ridley, A.J. (2001). Rho GTPases and cell migration. *J. Cell Sci.* 114, 2713–2722.
- Ridley, A.J., Schwartz, M.A., Burridge, K., Firtel, R.A., Ginsberg, M.H., Borisy, G., Parsons, J.T., and Horwitz, A.R. (2003). Cell migration: integrating signals from front to back. *Science* 302, 1704–1709.
- Rivero, F., Koppel, B., Peracino, B., Bozzaro, S., Siegert, F., Weijer, C.J., Schleicher, M., Albrecht, R., and Noegel, A.A. (1996). The role of the cortical cytoskeleton: F-actin crosslinking proteins protect against osmotic stress, ensure cell size, cell shape and motility, and contribute to phagocytosis and development. *J. Cell Sci.* 109, 2679–2691.
- Roberts, M.S., Woods, A.J., Dale, T.C., van der Sluijs, P., and Norman, J.C. (2004). Protein kinase B/Akt acts via glycogen synthase kinase 3 to regulate recycling of $\alpha\beta 3$ and $\alpha 5 \beta 1$ integrins. *Mol. Cell Biol.* 24, 1505–1515.
- Scheid, M.P., and Woodgett, J.R. (2001). PKB/AKT: functional insights from genetic models. *Nat. Rev. Mol. Cell Biol.* 2, 760–768.
- Sechi, A.S., and Wehland, J. (2000). The actin cytoskeleton and plasma membrane connection: PtdIns(4,5)P₂ influences cytoskeletal protein activity at the plasma membrane. *J. Cell Sci.* 113, 3685–3695.
- Servant, G., Weiner, O.D., Herzmark, P., Balla, T., Sedat, J.W., and Bourne, H.R. (2000). Polarization of chemoattractant receptor signaling during neutrophil chemotaxis. *Science* 287, 1037–1040.
- Small, J.V., Stradal, T., Vignal, E., and Rottner, K. (2002). The lamellipodium: where motility begins. *Trends Cell Biol.* 12, 112–120.
- Stossel, T.P., Condeelis, J., Cooley, L., Hartwig, J.H., Noegel, A., Schleicher, M., and Shapiro, S.S. (2001). Filamins as integrators of cell mechanics and signalling. *Nat. Rev. Mol. Cell Biol.* 2, 138–145.
- Takahashi, M. (2001). The GDNF/RET signaling pathway and human disease. *Cytokine Growth Factor Rev.* 12, 361–373.
- Usukura, J. (1993). Rapid freezing and subsequent preparation methods in retinal cell biology. In *Methods in Neurosciences*, P.A. Hargrave, ed. (San Diego: Academic Press, Inc.), pp. 37–53.
- Vanhaesebroeck, B., Leever, S.J., Ahmadi, K., Timms, J., Katso, R., Driscoll, P.C., Woscholski, R., Parker, P.J., and Waterfield, M.D. (2001). Synthesis and functions of 3-phosphorylated inositol lipids. *Annu. Rev. Biochem.* 70, 535–602.
- Vivanco, I., and Sawyers, C.L. (2002). The phosphatidylinositol 3-kinase-Akt pathway in human cancer. *Nat. Rev. Cancer* 2, 489–501.
- Watanabe, T., Wang, S., Noritake, J., Sato, K., Fukata, M., Takefuji, M., Nakagawa, M., Izumi, N., Akiyama, T., and Kaibuchi, K. (2004). Interaction of IQGAP1 links APC to Rac1, Cdc42, and actin filaments during cell polarization and migration. *Dev. Cell* 7, 871–883.
- Yoshimura, T., Kawano, Y., Arimura, N., Kawabata, S., Kikuchi, A., and Kaibuchi, K. (2005). GSK-3 β regulates phosphorylation of CRMP-2 and neuronal polarity. *Cell* 120, 137–149.
- Zhou, G., Zhuo, Y., King, C.C., Fryer, B.H., Bokoch, G.M., and Field, J. (2003). Akt phosphorylation of serine 21 on Pak1 modulates Nck binding and cell migration. *Mol. Cell Biol.* 23, 8058–8069.

Accession Numbers

The human Girdin cDNA sequence has been deposited in GenBank/EMBL/DBJ with the accession number AB201172.

Phosphorylation by Rho Kinase Regulates CRMP-2 Activity in Growth Cones

Nariko Arimura,^{1,2} Céline Ménager,¹ Yoji Kawano,^{1,5} Takeshi Yoshimura,¹
Saeko Kawabata,¹ Atsushi Hattori,¹ Yuko Fukata,¹ Mutsuki Amano,¹
Yoshio Goshima,³ Masaki Inagaki,² Nobuhiro Morone,⁴
Jiro Usukura,⁴ and Kozo Kaibuchi^{1*}

Department of Cell Pharmacology, Graduate School of Medicine, Nagoya University, 65 Tsurumai, Showa, Nagoya, Aichi 466-8550, Japan¹; Division of Biochemistry, Aichi Cancer Center Research Institute, 1-1 Kanokoden, Chikusa, Nagoya, Aichi 464-8681, Japan²; Department of Molecular Pharmacology and Neurobiology, Yokohama City University School of Medicine, 3-9 Fukuura, Kanazawa, Yokohama 236-0004, Japan³; Department of Anatomy, School of Medicine, Nagoya University, 65 Tsurumai, Showa, Nagoya, Aichi 466-8550, Japan⁴; and Division of Molecular and Cell Biology, Institute for Medical Science, Dokkyo University School of Medicine, 880 Kitakobayashi, Mibumachi, Tochigi 321-0293, Japan⁵

Received 18 May 2005/Returned for modification 27 June 2005/Accepted 29 August 2005

Collapsin response mediator protein 2 (CRMP-2) enhances the advance of growth cones by regulating microtubule assembly and Numb-mediated endocytosis. We previously showed that Rho kinase phosphorylates CRMP-2 during growth cone collapse; however, the roles of phosphorylated CRMP-2 in growth cone collapse remain to be clarified. Here, we report that CRMP-2 phosphorylation by Rho kinase cancels the binding activity to the tubulin dimer, microtubules, or Numb. CRMP-2 binds to actin, but its binding is not affected by phosphorylation. Electron microscopy revealed that CRMP-2 localizes on microtubules, clathrin-coated pits, and actin filaments in dorsal root ganglion neuron growth cones, while phosphorylated CRMP-2 localizes only on actin filaments. The phosphomimic mutant of CRMP-2 has a weakened ability to enhance neurite elongation. Furthermore, ephrin-A5 induces phosphorylation of CRMP-2 via Rho kinase during growth cone collapse. Taken together, these results suggest that Rho kinase phosphorylates CRMP-2, and inactivates the ability of CRMP-2 to promote microtubule assembly and Numb-mediated endocytosis, during growth cone collapse.

Axon guidance is essential for the complexity of brain circuitry. Growth cones are thought to be a sensor for guidance molecules during development. Growth cones localize at the tips of axons and dynamically change their morphology in response to attractive and repulsive guidance cues, thus determining the direction of growth (16). Such morphological changes in growth cones are thought to be achieved by cytoskeleton reorganization, cell adhesion, and endocytosis (55, 64). Growth cones consist of actin filaments at the edge and microtubules and neurofilaments at the center. Recently, it was revealed that actin filaments are regulated during growth cone collapse induced by repulsive guidance cues (23). Furthermore, microtubules and endocytosis regulate growth cone morphology (11, 18, 26, 30, 43, 51). However, signal cascades regulating microtubules and endocytosis remain to be clarified.

Recent evidence supports the idea that cytoskeletal components are required for proper axonal path finding, and these components are regulated by members of the Rho family, including RhoA, Rac1, and Cdc42 (32, 36). Rho proteins serve as molecular switches by cycling between an inactive GDP-bound state and an active GTP-bound state (35, 42). In their active state, these GTPases bind characteristic sets of effector

proteins. The most important effector of RhoA in the growth cone is probably the serine-threonine kinase, Rho-associated kinase (Rho kinase)/ROK α /ROCKII (5, 9, 74). Rho kinase binds to and is activated by the GTP-bound active form of Rho (2, 40).

Several research groups, including ours, support the idea that Rho kinase is a negative regulator of neurite formation and growth cone motility in neuronal cells downstream of Rho (1, 5, 38, 71). The ephrins, ligands of Eph receptor tyrosine kinases, have also been reported as a repulsive guidance cue to activate the Rho/Rho kinase signaling cascade during growth cone collapse (13, 71). The roles of the Eph family and ephrins in axon guidance have been studied in topographically organized sensory systems such as the retinotectal projection (21, 24, 46, 72). Activation of Eph receptor by, for example, ephrin-A5 causes the turning or collapse of growth cones. Analysis of the underlying signaling cascade has led to the identification of signaling molecules, such as ephexin, a Rho-specific guanine nucleotide exchange factor, which directly binds to Eph receptor and mediates signal from receptor to RhoA (44, 61, 63). In addition, myosin light chain (MLC) has been identified as one of the major substrates of Rho kinase-mediated growth cone collapse (1, 71). However, it is still unknown whether MLC phosphorylation is sufficient to mimic growth cone collapse induced by extracellular signals such as ephrin-A5 (71).

We previously identified collapsin response mediator protein 2 (CRMP-2) as a substrate of Rho kinase in the brain (5).

* Corresponding author. Mailing address: Department of Cell Pharmacology, Graduate School of Medicine, Nagoya University, 65 Tsurumai, Showa, Nagoya, Aichi 466-8550, Japan. Phone: 81 52 744 2074. Fax: 81 52 744 2083. E-mail: kaibuchi@med.nagoya-u.ac.jp.

CRMP-62, the chick CRMP-2 (98% identity), is reported to be required for the growth cone collapse of dorsal root ganglion (DRG) neurons induced by a repulsive guidance cue, semaphorin-3A (Sema3A; also known as collapsin-1) (30). UNC-33, the *Caenorhabditis elegans* homologue (30% homology), is identified by a mutation resulting in severely uncoordinated movement, abnormalities in axon guidance, and a superabundance of microtubules in neurons (37, 49). These results indicate that CRMP-2 is also a major mediator of growth cone collapse induced by repulsive guidance cues. We and other groups have reported that CRMP-2 is phosphorylated by Cdk5 and GSK-3 β downstream of Sema3A (10, 14, 68, 73). This phosphorylation of CRMP-2 is essential for Sema3A-induced growth cone collapse (10). However, the exact roles of CRMP-2 phosphorylation remain to be clarified.

We recently identified two molecules, tubulin heterodimer and Numb, as CRMP-2-interacting molecules (28, 34). CRMP-2 shows much higher affinity to tubulin heterodimers than the polymerized tubulin (microtubules). CRMP-2 copolymerizes with tubulin dimers into microtubules and promotes tubulin polymerization in vitro. Furthermore, the overexpression of CRMP-2 facilitates the rate of axonal growth, whereas the mutant lacking the activity of the microtubule assembly inhibits axonal growth. Given the enriched localization of CRMP-2 in growing axons, it is likely that the CRMP-2-tubulin complex concentrated in the distal part of the axon promotes microtubule assembly and axon formation (28). CRMP-2 participates in Numb-mediated endocytosis and regulates L1 recycling at the growth cone, followed by axon elongation (56). Thus, CRMP-2 basically has positive effects on axon growth. These results raise the possibility that modification, such as phosphorylation, of CRMP-2 regulates the CRMP-2 activity in axon growth or growth cone dynamics, including growth cone collapse.

Here, we report that phosphorylation by Rho kinase diminishes the CRMP-2 activity with respect to binding to tubulin dimer and Numb in neurons. Such phosphorylation by Rho kinase is observed during ephrin-A5-induced growth cone collapse. These results suggest that phosphorylation of CRMP-2 by Rho kinase enhances growth cone collapse by inhibiting the ability of CRMP-2 to associate with microtubules and Numb.

MATERIALS AND METHODS

Materials and chemicals. cDNA encoding human CRMP-2 was obtained as described previously (5). CRMP-2 was subcloned into pB-GEX (rearranged vector from pGEX) or pRSET-C1 (Invitrogen Corp., Carlsbad, CA) to obtain the construct of CRMP-2 with glutathione S-transferase (GST) tagged at the C terminus of the protein or with His tagged at the N terminus of the protein. pEF-ephrin-A5/RAGS-Fc was kindly provided by Hideaki Tanaka (Kumamoto University) (57). The following antibodies were used: anti-CRMP-2 monoclonal antibody (C4G), kindly provided by Yasuo Ihara (Tokyo University) (33); anti-CRMP-2 polyclonal antibody raised against GST-CRMP-2; anti-phospho-CRMP-2 antibody (pT555 and pT514) raised against chemically synthesized phosphopeptides which are exactly identical to the amino acid sequence of chick CRMP-2, namely, CRMP-62 (5, 31, 73); anti-GST polyclonal antibody raised against GST; anti-Numb polyclonal antibody raised against 20-amino-acid residues at the C terminus of Numb; anti-myc polyclonal antibody (Santa Cruz Biotechnology Inc., CA); anti-Rho-GDI polyclonal antibody (Santa Cruz); anti-actin monoclonal antibody (clone C4; Chemicon International, Temecula, Calif.); anti- α -tubulin monoclonal antibody (DM1A; Sigma, St. Louis, MO); and anti-unique β -tubulin monoclonal antibody (TUJ1; Berkeley Antibody Company, Berkeley, CA). N1E-115 cells were kindly provided by Taiji Kato (Nagoya City University Medical School, Nagoya, Japan). Vero cells were kindly provided

by Eisuke Mekada (Osaka University, Osaka, Japan). Y-27632 was provided by Mitsubishi Pharma Co. (Osaka, Japan). Other materials and chemicals were obtained from commercial sources.

Protein purification. Tubulin heterodimer was prepared from bovine brain by three cycles of polymerization and depolymerization followed by DEAE-Sepharose column chromatography using fast protein liquid chromatography (Amersham Biosciences Corp., Piscataway, NJ). Native bovine CRMP-2 was purified from bovine brain extracts by a method described previously (5). His-tagged CRMP-2 and GST-tagged CRMP-2 (CRMP-2-GST) were purified following the procedures recommended by Invitrogen Corp.

Phosphorylation assay. The phosphorylation assay of the samples was carried out as described previously (52). In brief, the kinase reaction for Rho kinase was performed in 50 μ l of a reaction mixture (102 mM PIPES at pH 6.8, 1 mM EDTA, 1 mM dithiothreitol, 1.55 mM MgSO₄, 100 μ M [γ -³²P]ATP [1 to 20 GBq/ μ mol], 100 nM purified GST-Rho kinase catalytic domain [RhoK-cat]) for 30 min at 30°C. RhoK-cat was produced in Sf9 cells with a baculovirus system and purified on glutathione-Sepharose 4B beads (Amersham Biosciences Corp.). GSK-3 β and Cdk5 were obtained from Upstate Biotech (Charlottesville, VA). Then, the reaction mixtures were boiled in sodium dodecyl sulfate (SDS) sample buffer and subjected to SDS-polyacrylamide gel electrophoresis (SDS-PAGE) for estimation of the stoichiometry. The radiolabeled bands were visualized by an image analyzer (BAS 2000; Fujifilm, Tokyo, Japan).

In vitro binding assay. We first immobilized 0.5 μ M phosphorylated or non-phosphorylated CRMP-2 onto glutathione-Sepharose 4B beads for 60 min at 4°C. To examine the interaction of CRMP-2 and tubulin heterodimers, the immobilized CRMP-2 with beads was incubated with 1.0 μ M tubulin heterodimer for 120 min at 4°C. After removal of the supernatant of the CRMP-2-tubulin mixture, the beads were washed three times with PEM buffer (100 mM PIPES at pH 6.8, 1 mM EGTA, 0.5 mM MgSO₄). Then the samples were boiled in SDS sample buffer and subjected to SDS-PAGE and immunoblot analysis with the indicated antibodies. To examine the interaction of CRMP-2 with other molecules, the immobilized CRMP-2 was incubated with rat brain (P6 and P7) lysate in lysis buffer (20 mM Tris-HCl at pH 8.0, 150 mM NaCl, 1 mM EDTA, 1 mM phenylmethylsulfonyl fluoride, 10 μ g/ml leupeptin, 10 μ g/ml aprotinin, 1.0% NP-40, 1 μ M calyculin A) for 60 min at 4°C. After removal of the supernatant, the beads were washed three times with washing buffer (20 mM Tris-HCl at pH 8.0, 150 mM NaCl, 1 mM EDTA, 1.0% NP-40). Then the samples were boiled in SDS sample buffer and subjected to SDS-PAGE and immunoblot analysis with the indicated antibodies.

Surface plasmon resonance measurements. Anti- α -tubulin monoclonal antibody (DM1A) was covalently coupled to a CM5 sensor chip in a Biacore 3000 system (Biacore, Tokyo, Japan) according to the manufacturer's instructions. Purified tubulin heterodimer (0.5 μ M) was captured at a flow rate of 10 μ l/min for 3 min. The level of resonance units raised by the addition of anti-tubulin antibodies was about 1,800 to 2,000 in each condition. Binding of 8, 4, 2, 1, and 0.5 μ M phosphorylated or nonphosphorylated His-CRMP-2 to a sensor chip surface loaded with tubulin heterodimer was done in 100 mM PIPES (pH 6.8)–150 mM NaCl–3 mM EDTA–0.005% (wt/vol) Tween 20. Injection of each sample was programmed separately. Association was monitored over 3 min at a flow rate of 20 μ l/min. The data were analyzed with the BIAevaluation 3.0 software (Biacore).

Cosedimentation assay. Tubulin (10 μ M) was first assembled with 1 mM GTP, 10% dimethyl sulfoxide, and 20 μ M Taxol for 30 min at 37°C. The assembled microtubules were mixed with 5 μ M bovine serum albumin (BSA) or 5 μ M phosphorylated or nonphosphorylated His-tagged CRMP-2 in PEM buffer. This mixture was incubated at 37°C for 10 min and centrifuged at 100,000 \times g for 10 min at 37°C. The pellet and supernatant were subjected to SDS-PAGE.

Cell culture and transfection. Vero cells and N1E-115 cells were seeded on 13-mm round glass coverslips at 1.5×10^4 cells/mm² for immunostaining and cultured in Dulbecco's modified Eagle's medium containing 10% fetal bovine serum in an atmosphere of 5% CO₂ at 37°C. For transfection, Vero and N1E-115 cells were seeded and cultured overnight. Transfection of plasmids was carried out using Lipofectamine 2000 (Invitrogen) for Vero cells or Lipofectamine (Invitrogen) for N1E-115 cells. Chick DRG neurons were dissociated from 7-day-old chick embryos by use of papain as described previously (8). They were then seeded on 13-mm round glass coverslips coated with laminin at 1.5×10^4 cells/mm² in 24-well plates for immunostaining or on 35-mm culture dishes coated with laminin at 1.5×10^4 cells/mm² for immunoblot analysis. The cells were cultured in Dulbecco's modified Eagle's medium containing 100 ng/ml 2.5S nerve growth factor (NGF; Upstate Biotech) and 10% fetal bovine serum in an atmosphere of 5% CO₂. DRG neurons were prepared and transfected with the indicated plasmids by use of the calcium phosphate method before plating, as described previously (5). The transfection efficiency is about 1 to 2% using the